AN IN VITRO ASSAY FOR ACUPUNCTURE: EFFECTS OF GEL COMPOSITION, PROPERTIES, AND GEOMETRY ON THE ALIGNMENT RESPONSE

by

MARGARET JULIAS

A dissertation submitted to the

Graduate School-New Brunswick

Rutgers, The State University of New Jersey

in partial fulfillment of the requirements

for the degree of

Doctor of Philosophy

Graduate Program in Chemical and Biochemical Engineering

written under the direction of

David I. Shreiber

and approved by

_____

_____

_____

_____

New Brunswick, New Jersey

January 2010

ABSTRACT OF THE DISSERTATION

AN IN VITRO ASSAY FOR ACUPUNCTURE: EFFECTS OF GEL COMPOSITION, PROPERTIES, AND GEOMETRY ON THE ALIGNMENT RESPONSE

By MARGARET JULIAS

Dissertation Director:
David I. Shreiber

Acupuncture is a traditional Eastern therapy that is increasingly used as an alternative therapy in the United States, but remains poorly understood. During acupuncture, needles are inserted subcutaneously at specific acupuncture points and rotated to achieve “de qi”, a warming sensation felt by the patient, which to the therapist coincides with a grasping resistance to further needle manipulation. Research has demonstrated that needle grasp results specifically from loose fascial connective tissues winding around the needle, and that needle grasp is stronger at acupuncture points, which fall above intermuscular fascial planes, than other locations on the body. To determine if mechanical stimulation is related to the therapeutic benefits of acupuncture, the features that govern the enhanced mechanical coupling need to be understood, but this is difficult to evaluate in vivo or in situ. In this thesis, several of these features are examined in a controlled, in vitro setting using collagen gels as the basis. The thickness, concentration, mechanical properties, size, shape, and composition of collagen gels were systematically altered, and the response to controlled acupuncture evaluated by capturing the evolution of fiber

alignment using polarized light microscopy. Alignment was observed to increase with increasing collagen concentration, but decrease when the collagen was stiffened via crosslinking. Crosslinked gels failed after fewer rotations than untreated gels. Alignment was increased with increasing depth of insertion, but decreased in thicker gels when needle depth was held constant. Collagen gels cast in ellipses or strips to mimic fascial plane anatomy resisted failure and aligned more readily than circular gels. Alignment in these gels was anisotropic, with stronger alignment across the ellipse or plane, and entrapped rat fibroblasts followed the alignment pattern. The inclusion of fibrin in a composite gel with collagen significantly increased the ability of the gel to withstand needle rotations, which ultimately generated significantly greater alignment. The addition of hyaluronic acid produced less dramatic effects. Connective tissue is uniquely structured and organized to enable specific and substantial mechanical interactions during acupuncture. The in vitro system can be expanded to study cellular responses for understanding of underlying biological mechanisms and subsequent engineering applications.

DEDICATION

To my family

ACKNOWLEDGEMENT

I am writing this acknowledgement after the fact that I have presented my thesis presentation on December 21, 2009. I can not remember every single detail of what went on that day. Everyone that went through the process knows the emotional roller coaster during the week of the defense. I would like to thank everyone for being there. I also would like to acknowledge the committee members. The dissertation defense will not be possible without them. I want to thank Henrik Pedersen and Michael G. Dunn for being part of the committee members. I would especially like to thank my amazing advisors Helen M. Buettner and David I. Shreiber.

I want to thank Helen for believing in me. I'm a chemical engineer by nature, so naturally biology is not one of my stronger elements. When Helen presented the acupuncture project to the first year students, including me, the project caught my attention. With only high-school biology background, I went and asked her about being part of the acupuncture project. I'm glad I aced her analytical method class; otherwise, I probably would not have the courage to approach her. I really like to thank her for being such a great mentor and standing by me over these years and being patient with me even with the slow start. I really look up to her and I hope I can be as good as her someday.

I also want to thank Dave for putting up with me all this years. I remember the first time I met him in his office. His personality is quite the opposite of Helen's. I was always nervous around him, and he easily made me doubt myself. If he asked me whether I was

sure about “1+1 = 2”, my answer would be no. Overtime, because of his guidance, I gained confidence in what I do. Although comments from Dave can be hurtful sometime, it is only because he cares so much about his students. I hope I did not disappoint him and more importantly did not “sink” the project. I especially want to thank him for the past few weeks before the defense. I don’t think I could have finished the thesis without his help.

Furthermore, I want to thank my proposal committee members: Martin Yarmush, Yee Chiew, and Mourad Bouzit. I also want to acknowledge Deanna Thompson, Alice Seneres, Lowell T. Edgar, Uday Chippada, and John Petrowski for helping me during this program. It has been a grueling process, and the past two years had been harder than ever. I want to thank my best friend Patricia Brieva and the following friends/lab mates: Kapo Chu, Ian Gaudet, Chris Gaughn, Jeremy Griffin, Frank Jiang, Shirley Masand, Gary Monteiro, Mohammad Sadik, Minjung Song, Harini Sundararaghavan, and Jing Xu. My life at Rutgers would be so much different without them. They provided me with a great docking station.

Finally, I want to thank my beloved sister for being there for me through these years. She helped me and provided me with anything I need. She rather had no sleep and helped me with things that she would not even get credit for. She is the greatest sister and the best roommate ever. I also want to thank my awesome brother for always taking all the “bad” and giving all the “best”. All this time, he took responsibility of me and my sister. If I need someone I can count on, I know he is the one. Lastly, I want to thank my parents.

There is nothing I need to do to make them love me even more. Mom, Dad, my sister and my brother, you are the rock of my life.

TABLE OF CONTENTS

LISTS OF TABLES

LIST OF ILLUSTRATIONS

CHAPTER 1: INTRODUCTION

1.1 Background

Acupuncture is a therapeutic practice originating in China more than 2000 years ago. Over 3 million adults have experienced acupuncture, where its use is increasingly common in the United States [1, 2]. Acupuncture has been shown effective in treating pain, nausea, and hypertension [1, 3]. The growing popularity of acupuncture reflects an interest on the part of the public in alternatives to conventional medicine that offer fewer side effects and that may be more effective in treating certain conditions [4, 5]. As with any treatment, medical evidence is important, not only to validate acupuncture therapy but also to understand the full range of its possible applications.

Despite centuries of practice, little is understood scientifically about how acupuncture works. Most studies have assumed that acupuncture effects occur via the nervous system. However, recent in vivo and ex vivo studies results indicate that acupuncture may also involve local tissue effects that have been overlooked in neurophysiological studies [6]. Traditionally, acupuncture treatments involve the insertion of fine needles into specific locations on the body known as acupuncture points. The needle is then manipulated by rotating or pistoning to elicit “de qi.” De qi is an essential characteristic in the therapeutic application of acupuncture resulting in a measurable biomechanical phenomenon known as “needle grasp”, which can be quantified by measuring the force necessary to remove the acupuncture needle [7, 8].

Studies show that needle grasp involves specific coupling of subcutaneous tissue to the needle and not skeletal muscle contraction [6]. Acupuncture needling and manipulation causes alignment and deformation of subcutaneous connective tissue surrounding the needle. For instance, rotating acupuncture needles – which is the most often employed manipulation in clinical therapy – causes the subcutaneous connective tissue to wind around the needle and draw neighboring connective tissue inward. Mechanical stress as a result of acupuncture needling has been shown to cause a change in cell morphology, where the extent of change depends on the degree of needle manipulation [9-11]. Tissue deformation and alignment may send mechanical signals to residing cells, which may then be translated to locations remotely from the point of origin through the dendritic network of fibroblasts [12].

Nevertheless, the role of the cellular network within connective tissues and the changes that occur in these tissues following acupuncture, such as expanded cell morphology, remain to be elucidated. Mechanical signals felt by fibroblasts may activate multiple signaling cascades leading to cellular responses such as cell contraction, migration, protein synthesis, and cellular effects including cell proliferation, cell survival, cell differentiation, and cell death due to modification of the surrounding ECMs [6, 13]. These events may further affect neighboring cells and the surrounding matrix, resulting in further remote effects. Understanding acupuncture therapy in its entirety requires an understanding of the mechanism and effects of needling, including effects at the local tissue level.

1.2 Acupuncture Points

The human body includes at least 2,000 acupuncture points, of which about 150 are most commonly used. Applying therapy to the different points can produce varying therapeutic effects [14]. Due to high interests in acupuncture [2, 3], many studies were done clinically mainly to show acupuncture efficacy. However, most studies remained inconclusive due to poor methodology [3]. It is difficult to prevent patients from feeling the needle insertion. Since the acupuncture points are connected through meridians within the body, some believe acupuncture works on a neuronal level to explain the distant effect from stimulation point. However, the physiological, anatomical, or neurophysiological significance of acupuncture points has not yet to be fully understood. Hence, the mechanism behind acupuncture therapy remains unclear.

Nevertheless, Dr. Langevin's work provided us with some insights. Needling at acupuncture points creates greater pull out force than needling at other locations [7]. As mentioned, studies showed that needle grasp involved mainly subcutaneous tissue and not skeletal muscle contraction [6]. Since many (~80%) acupuncture points fall on a fascial plane [8], which contains a higher connective tissue content that led to greater needle-connective tissue contact and mechanical coupling [7, 8]. However, needling at non-acupuncture points (control) also resulted in needle grasp [7]. Placebo effects from patients experiencing the needle insertions might also originate from minor responses at control points. Indeed, many clinical studies prove to be inconclusive [3], and the coupling at control points may confound the results.

Hence, there is a need to have a system that enables the study of acupuncture therapy without the complication of improper control. In vivo and ex vivo observations indicate that acupuncture needling causes changes in extracellular matrix organization and architecture, specifically, alignment of connective tissue fibers in the direction of needle rotation [6, 13]. It is believed that tissue deformation sends mechanical signals to residing cells that may result in cascading cellular responses [6, 13]. Nevertheless, the significance of the location of acupuncture points and whether acupuncture points fall on fascial planes is merely a coincidence or a tool to propagate mechanical signals is an immediate question.

1.3 Elements of Acupuncture

As mentioned, there is strong evidence that connective tissue is uniquely involved during application of acupuncture, at least mechanically if not therapeutically. Winding of connective tissue in a whorl pattern was visualized using ultrasound scanning and histochemical staining [6]. The histological examination also showed denser subcutaneous connective tissue around the needled area [6]. Deformation of connective tissues is believed to be due mainly to extracellular matrix fibers winding around the needle during the needle rotation. Tissue winding, which produces needle grasp, was found enhanced at acupuncture points [7]. Thus, although the downstream effects of the mechanical interactions between needles and connective tissues and the relationship of those effects to the therapeutic benefits associated with acupuncture are largely unknown, there are clearly unique features of connective tissue and/or acupuncture points that enable this enhanced mechanical stimulation.

1.3.1 Connective tissue

As needling was done through dermis, subcutaneous muscles, subcutaneous connective tissues, and into muscle layers, only connective tissues showed winding and tissue thickening [13]. The specificity of connective tissue winding excluding the rest of tissue layers suggest that there are aspects of it structure, composition, and/or properties that distinguish it from neighboring tissues.

In general, mammalian connective tissue consists mainly of fibrillar type I collagen, which forms fibril bundles that contribute to the tissue microarchitecture (Christiansen and Silver 1999). The mechanical properties of connective tissue vary depending on the collagen fiber size, collagen density, content of collagen, and other components within the connective tissue, including elastic fibers, proteoglycans, and resident cells. In addition, the connective tissue properties are affected by variables such as the age, nutrition, and location in the body. Aging of connective tissues, an unpreventable event, will change ECM structure, composition, density, and mechanical properties [15]. Structurally, loose connective tissue maintains a much sparser network of fibers than other connective tissues, such as dermis. Mechanically, this results in unique properties.[16] showed that unlike dermis, which demonstates hyperelastic strain-stiffening behavior typical of collagen-dense tissues (like tendons and ligaments), loose connective tissue presents largely linearly elastic behavior. How these properties influence mechanical interactions during needling are unknown, and difficult to untangle in an in vivo or in situ setting.

1.3.2 Acupuncture points

While connective tissue appears to specifically interact with acupuncture needles during therapeutic manipulations, the interactions are stronger at traditional acupuncture points than 'control' points. These points are mostly (80%) located at fascial planes and 50% of them coincide with the meridians [8]. At these planes, there is a relative abundance of loose connective tissue, which may offer more tissue for interactions, and there are also distinct boundary conditions when compared to loose connective tissue located superficial to skeletal muscles. At fascial planes, connective tissue is bounded on two sides by skeletal muscle, and the width of the plane narrows with increasing depth. Elsewhere, the tissue is largely unbounded. As with connective tissue properties, it is difficult to decouple aspects of the anatomical organization of the tissues in vivo or in explant models. We believe through an in vitro system, we are able to have a system that enables the study of these acupuncture elements in better controlled and quantitative manners.

1.4 In Vitro Systems

Of course, in vivo environments provide tissues with a complex and balanced set of biochemical, mechanical, and electrical signals that regulate cell function. These signals come from extracellular matrix contacts as well as autocrine, paracrine and endocrine pathways. Thus, in vivo systems consist of multiple, simultaneous processes involving multiple cell types. On the other hand, in vitro systems reduce the degree of complexity in the experimental system, providing simplified versions of cells' native surroundings to

maintain cell viability, growth, and certain limited cell-specific functions [17]. The simplified in vitro environment allows specific studies at the molecular, cellular and tissue level that would be difficult or impossible to study in vivo.

Indeed, the basic components of loose connective tissue – type 1 collagen and fibroblasts – are easily incorporated into 3D in vitro assays. Fibrillar collagen gels has been used to understand some of the basic elements of tissue biomechanics and cell-matrix interactions [18-28]. For instance, fibroblast-populated collagen lattices (FPCL) are frequently used as basis for in vitro assays of wound healing [29, 30], and as a platform for tissue engineering [31], as the 3D environment collagen environment provides a more relevant yet controllable platform to study cell morphology, protein synthesis, degradation of connective tissue components and the cell response to growth factors [18, 20].

A 3D in vitro assay would enable the modification of the 'tissue' components, properties, concentrations, and dimensions, which can be controlled and designed to measure the parameters of interest. In this project, the initial assays consisted of the primary components of connective tissue, i.e., collagen and fibroblasts. These assays can subsequently refined by the addition of other components to mimic the complexity of connective tissue and improve the in vitro representation of in vivo conditions. In this thesis, we develop a 3D in vitro system to address the response of loose connective tissue to acupuncture needle rotation.

1.5 Summary

Acupuncture needle rotation causes two observable tissue effects: 1) subcutaneous connective tissue deformation in a whorl pattern around the acupuncture needle, and 2) needle grasp, a measurable biomechanical resistance to needle removal [6, 8]. Deformation of connective tissues is believed to be the result of extracellular matrix fibers winding around the needle during the needle rotation. Since collagen and fibroblasts are the major fibrous and cellular components in connective tissue, respectively, an in vitro system consisting of collagen and fibroblasts can be used to represent the local connective tissue around the needled area.

We believe that the unique location, composition, geometry, and other properties of loose connective tissue may contribute the mechanical coupling and transmission of force during acupuncture needling, which may lead to therapeutic effects. Studying these aspects in a controlled setting in vivo or in situ is extremely difficult. Fundamentally, they can be recapitulated in an in vitro model. In this thesis, we develop an in vitro system that mimics the feature of connective tissue in a controlled a quantitative setting. In the following chapter (chapter 3), we introduce the model and study the effects of needling parameters and tissue mechanical properties on the tissue mimic's response. In chapter 4, we examine the role of geometric boundary conditions on the alignment and mechanical failure of the mimics. In chapter 5, we assess the influence of tissue composition on the response to needling. Finally, in chapter 6, we summarize and synthesize these results and suggest future directions to further elucidate the role of mechanics in acupuncture.

1.6 References

1. Statement, N.C., *Acupuncture*. 1997, NIH.
2. Pleis, J.R. and J.W. Lucas, *Summary health statistics for U.S. adults: National Health Interview Survey, 2007.* Vital Health Stat 10, 2009(240): p. 1-159.
3. Birch, S., et al., *Clinical research on acupuncture. Part 1. What have reviews of the efficacy and safety of acupuncture told us so far?* J Altern Complement Med, 2004. **10**(3): p. 468-80.
4. Eisenberg, D., et al., *Trends in alternative medicine use in the United States, 1990-1997.* JAMA, 1998. **280**(18): p. 1569-1575.
5. Peleg, R., et al., *Patterns of Use of Nonbiomedical Medicine Services by Nonbiomedical Medicine Providers.* J Altern Complement Med, 2005. **11**(5): p. 917-921.
6. Langevin, H.M., et al., *Evidence of connective tissue involvement in acupuncture.* Faseb J, 2002. **16**(8): p. 872-4.
7. Langevin, H.M., et al., *Biomechanical response to acupuncture needling in humans.* J Appl Physiol, 2001. **91**(6): p. 2471-8.
8. Langevin, H.M. and J.A. Yandow, *Relationship of acupuncture points and meridians to connective tissue planes.* Anat Rec, 2002. **269**(6): p. 257-65.
9. Langevin, H.M., et al., *Dynamic fibroblast cytoskeletal response to subcutaneous tissue stretch ex vivo and in vivo.* Am J Physiol Cell Physiol, 2005. **288**(3): p. C747-56.
10. Langevin, H.M., et al., *Connective tissue fibroblast response to acupuncture: dose-dependent effect of bidirectional needle rotation.* J Altern Complement Med, 2007. **13**(3): p. 355-60.
11. Langevin, H.M., et al., *Fibroblast spreading induced by connective tissue stretch involves intracellular redistribution of alpha- and beta-actin.* Histochem Cell Biol, 2006. **125**(5): p. 487-95.
12. Langevin, H.M., C.J. Cornbrooks, and D.J. Taatjes, *Fibroblasts form a body-wide cellular network.* Histochem Cell Biol, 2004. **122**(1): p. 7-15.
13. Langevin, H.M., D.L. Churchill, and M.J. Cipolla, *Mechanical signaling through connective tissue: a mechanism for the therapeutic effect of acupuncture.* Faseb J, 2001. **15**(12): p. 2275-82.
14. Kaptchuk, T.J., *Acupuncture: theory, efficacy, and practice.* Ann Intern Med, 2002. **136**(5): p. 374-83.
15. Silver, F.H., D. DeVore, and L.M. Siperko, *Invited Review: Role of mechanophysiology in aging of ECM: effects of changes in mechanochemical transduction.* J Appl Physiol, 2003. **95**(5): p. 2134-41.
16. Iatridis, J.C., et al., *Subcutaneous tissue mechanical behavior is linear and viscoelastic under uniaxial tension.* Connect Tissue Res, 2003. **44**(5): p. 208-17.
17. Stegemann, J. and R. Nerem, *Phenotype modulation in vascular tissue engineering using biochemical and mechanical stimulation.* Annals of Biomedical Engineering, 2003. **31**(4): p. 391-402.
18. Bell, E., B. Ivarsson, and C. Merrill, *Production of a tissue-like structure by contraction of collagen lattices by human fibroblasts of different proliferative potential in vitro.* Proc Natl Acad Sci U S A, 1979. **76**(3): p. 1274-8.

19. Bride, J., et al., *Indication of fibroblast apoptosis during the maturation of disc-shaped mechanically stressed collagen lattices.* Arch Dermatol Res, 2004. **295**: p. 312-317.
20. Eckes, B., et al., *Downregulation of collagen synthesis in fibroblasts within three-dimensional collagen lattices involves transcriptional and posttranscriptional mechanisms.* FEBS, 1993. **318**(2): p. 129-133.
21. Elsdale, T. and J. Bard, *Collagen substrata for studies on cell behavior.* J Cell Biol, 1972. **53**(3): p. 626-637.
22. Girton, T., V. Barocas, and R. Tranquillo, *Confined compression of a tissue-equivalent: collagen fibril and cell alignment in response to anisotropic strain.* Journal of Biomechanical Engineering, 2002. **124**: p. 568-575.
23. Grinnell, F., *Fibroblast biology in three-dimensional collagen matrices.* Trends in Cell Biology, 2003. **13**(5): p. 264-269.
24. Grinnell, F., et al., *Dendritic fibroblasts in three-dimensional collagen matrices.* Molecular Biology of the Cell, 2003. **14**: p. 384-395.
25. Kessler, D., et al., *Fibroblasts in mechanically stressed collagen lattices assume a "synthetic" phenotype.* J Biol Chem, 2001. **276**(39): p. 36575-85.
26. Le, J., et al., *Production of matrix metalloproteinase 2 in fibroblast reaction to mechanical stress in a collagen gel.* Arch Dermatol Res, 2002. **294**(9): p. 405-10.
27. Mudera, V., et al., *Molecular responses of human dermal fibroblasts to dual cues: contact guidance and mechanical load.* Cell Motility and the Cytoskeleton, 2000. **45**: p. 1-9.
28. Ng, C.P. and M.A. Swartz, *Fibroblast alignment under interstitial fluid flow using a novel 3-D tissue culture model.* Am J Physiol Heart Circ Physiol, 2003. **284**(5): p. H1771-7.
29. Jing, Y. and Y. Jian-Xiong, *Human tissue factor pathway inhibitor-2 suppresses the wound-healing activities of human Tenon's capsule fibroblasts in vitro.* Mol Vis, 2009. **15**: p. 2306-12.
30. Murray, M.M., S.D. Martin, and M. Spector, *Migration of cells from human anterior cruciate ligament explants into collagen-glycosaminoglycan scaffolds.* J Orthop Res, 2000. **18**(4): p. 557-64.
31. Rowe, S.L. and J.P. Stegemann, *Interpenetrating collagen-fibrin composite matrices with varying protein contents and ratios.* Biomacromolecules, 2006. **7**(11): p. 2942-8.

CHAPTER 2: AN IN VITRO ASSAY OF COLLAGEN FIBER ALIGNMENT BY ACUPUNCTURE NEEDLE ROTATION

2.1 Abstract

Background: During traditional acupuncture therapy, soft tissues attach to and wind around the acupuncture needle. To study this phenomenon in a controlled and quantitative setting, we performed acupuncture needling in vitro. Methods: Acupuncture was simulated in vitro in three-dimensional, type I collagen gels prepared at 1.5 mg/ml, 2.0 mg/ml, and 2.5 mg/ml collagen, and either crosslinked with formalin or left untreated. Acupuncture needles were inserted into the gels and rotated via a computer-controlled motor at 0.3 rev/sec for up to 10 revolutions while capturing the evolution of birefringence under cross-polarization. Results: Simulated acupuncture produced circumferential alignment of collagen fibers close to the needle that evolved into radial alignment as the distance from the needle increased, which generally matched observations from published tissue explant studies. All gels failed prior to 10 revolutions, and the location of failure was near the transition between circumferential and radial alignment. Crosslinked collagen failed at a significantly lower number of revolutions than untreated collagen, whereas collagen concentration had no effect on gel failure. The strength of the alignment field increased with increasing collagen concentration and decreased with crosslinking. Separate studies were performed in which the gel thickness and depth of needle insertion were varied. As gel thickness increased, gels failed at fewer needle revolutions. For the same depth of insertion, alignment was greater in thinner gels. Alignment increased as the depth of insertion increased. Conclusions: These results indicate that the mechanostructural properties of soft connective tissues may affect

their response to acupuncture therapy. The in vitro model provides a platform to study mechanotransduction during acupuncture in a highly controlled and quantitative setting.

2.2 Background

In traditional acupuncture therapy, fine needles are inserted into the skin at specific points on the body and manipulated manually, typically by needle rotation. During this process, it is important to achieve the characteristic of “de qi”, a physical sensation experienced by the patient, and a biomechanical phenomenon experienced by the acupuncture therapist that is also known as needle grasp. In needle grasp, the therapist feels a resistance to further needle manipulation, which has been described as a fish biting on a line (see [1]). Recent studies by Langevin et al suggest that needle grasp results when collagen fibers of the loose, subcutaneous connective tissue couple to and wind around the rotating needle [2-4]. The connective tissue experiences significant deformation during this process. In addition, acupuncture needle manipulation in connective tissue explants induces cytoskeletal remodeling by fibroblasts [5, 6], the predominant cell type in loose connective tissue, supporting the hypothesis that tissue deformation due to needle manipulation mechanically stimulates fibroblasts, resulting in mechanotransduction effects that may contribute to therapeutic benefits [2, 3].

These in vivo and ex vivo findings have pioneered an exciting focus on connective tissue involvement in acupuncture, but also raise interesting questions about acupuncture needling and collagen fiber winding that motivate the need for in vitro tools. From a therapeutic perspective, if fiber winding does play an important role then parameters that affect winding would be expected to alter the therapeutic response. Candidate parameters

include ones that would affect tissue mechanics, such as matrix composition, density, and stiffness, as well as the thickness of the tissue layer(s). Identifying relationships among tissue properties, winding, and therapeutic effects through in vivo experiments alone, however, is complicated by normal in vivo variations in tissue properties. For example, the collagen content in skin is known to differ with location, tissue type, and skin layer [7-9]. Additionally, collagen content decreases with aging [10-12], potentially due to an increase in collagen crosslinking [13], and the thickness of the subcutaneous connective tissue is variable in humans, which may also affect the response to needling [14]. Accounting for these variations significantly increases the sample number required to obtain statistically meaningful in vivo data.

With this in mind, we have developed an in vitro approach to examine the first part of the proposed therapeutic mechanism, i.e., the link between tissue properties and collagen fiber winding, which can be used to guide further in vivo investigation. Specifically, we used type I collagen gels to study the effects of matrix properties on collagen fiber response to acupuncture needle rotation. We subjected gels with different collagen concentrations and degrees of crosslinking to computer-controlled needle rotation and used polarized light imaging to monitor the change in collagen fiber alignment during needle rotation. In separate gels, we varied the thickness and depth of needle insertion. Our results demonstrate that the winding response of fibrillar collagen to needle rotation resembles that of loose connective tissue and varies with network density and stiffness and the depth of needle insertion. The quantitative approach developed in this work provides a useful new tool to aid in elucidating tissue-level mechanisms of acupuncture.

2.3 Methods

2.3.1 Collagen gel preparation

Acellular collagen gels were prepared from lyophilized collagen (Elastin Products, Owensville, MO) as previously described [15]. A stock solution was prepared by dissolving 3.75mg/ml collagen in 0.02N acetic acid. The stock solution was diluted with 0.02N acetic acid, neutralized with 0.1N NaOH, and further diluted with M199 and 10XMEM media (Sigma Aldrich, St Louis, MO) to achieve the desired final collagen concentration of 1.5, 2.0, or 2.5mg/ml (see below). A 3-ml gel solution was poured into a 35-mm glass bottom MatTek dish with a 20-mm glass microwell (MatTek Corporation) and incubated at 37°C for 2hr to ensure complete fibril formation. After self assembly, 1ml of fresh phosphate buffered saline (PBS) was added on top of the gel. In some samples, the collagen solution was spiked with FITC-labeled collagen (Elastin Products, Owensville, MO) in a 1:9 ratio of fluorescent collagen:collagen to permit visualization of collagen fibers using confocal microscopy. For crosslinking studies, gels were incubated in 1ml of 10% neutral buffered formalin solution for 15 min on a rocker plate. The formalin solution was then replaced with PBS. The final height of gel was 4mm and did not vary significantly with crosslinking.

2.3.2 In vitro acupuncture

A computer-controlled motor (MicroMo Electronics, Inc.) was used to needle the collagen gels. A 250-μm stainless steel acupuncture needle (Seirin, Tokyo, Japan) was attached to the motor and inserted perpendicular to the surface of the gel to a depth of 3mm using a calibrated micromanipulator. The needle was rotated at 0.3rev/s for either 2

or 4 revolutions in samples used for confocal imaging, or for 10 revolutions in samples used for continuous recording of the evolution of fiber alignment with polarized light microscopy.

A separate series of experiments was performed to investigate the influence of the depth of needle insertion on the response of the gel. Collagen solution was prepared at 2.0mg/ml as described above, and gels were prepared such that the final gel height at the middle of the gel was 2mm, 4mm, or 6mm. These gels were subjected to in vitro acupuncture as described above, with the depth of needle insertion varying from 1.5mm to 4.5mm and 25%-75% of the thickness of the gel (Table 2-1).

Table 2-1: Conditions for investigating effects of needle insertion depth

Gel Height (mm)	Insertion Depth (mm)	Insertion Depth/Gel Height (%)
2	1.50	75.0
4	1.50	37.5
4	2.25	56.3
4	3.00	75.0
6	1.50	25.0
6	2.25	37.5
6	3.00	50.0
6	4.50	75.0

2.3.3 Confocal imaging

Confocal microscopy was used to examine the fibril alignment pre- and post- needle rotation. The MatTek dish was covered with a 3mm-thick sheet of poly(dimethyl siloxane) (PDMS), through which the acupuncture needle was inserted prior to entering the gel. The needle was rotated either 2 or 4 revolutions with the motor, after which the needle was de-coupled from the motor. Insertion through the PDMS prevented the needle

from recoiling when detached from the motor and allowed the transfer of the dish to the confocal microscope. The gel was imaged with a 63x objective using a laser wavelength of 488nm to visualize the fluorescent collagen fibers (excitation 497 nm, emission 520 nm). The confocal images were compared to bright field and polarized light images taken during the needling procedure.

2.3.4 Polarized light imaging

Polarization light microscopy (PLM) was used to observe and image the evolution of fiber alignment continuously in real time. A dissection stereomicroscope (Carl Zeiss Microimaging, Thornwood, NY) with a USB camera (Matrix Vision, GmbH, Oppenweiler, Germany) was physically inverted and clamped to a benchtop, such that the base of the microscope provided a platform to hold the motor stand and MatTek dish (Figure 2-1). A fiber-optic ring light (Edmund Optics, Barrington, NJ) was attached to the motor housing. The gel was placed between two polarizers, which were positioned as 'cross-polars' with their respective angles of polarization 90^{o} apart. In this arrangement, as the light passes through the filter-sample-filter optic train, the darkest area of the resulting image occurs where collagen fibers are oriented parallel or perpendicular to the optical axis of either polarizing element; the brightest area occurs where collagen fibers are oriented 45^{o} to the filter optical axis. The collagen gel was needled for 10 revolutions. Images were captured at 6 frames per second during needle rotation and were analyzed with MATLAB (The Mathworks, Inc, Natick, MA), as described below. Six experiments, each comprising three replicates, were performed for untreated collagen gels, and five experiments were performed for crosslinked gels, also in triplicate.

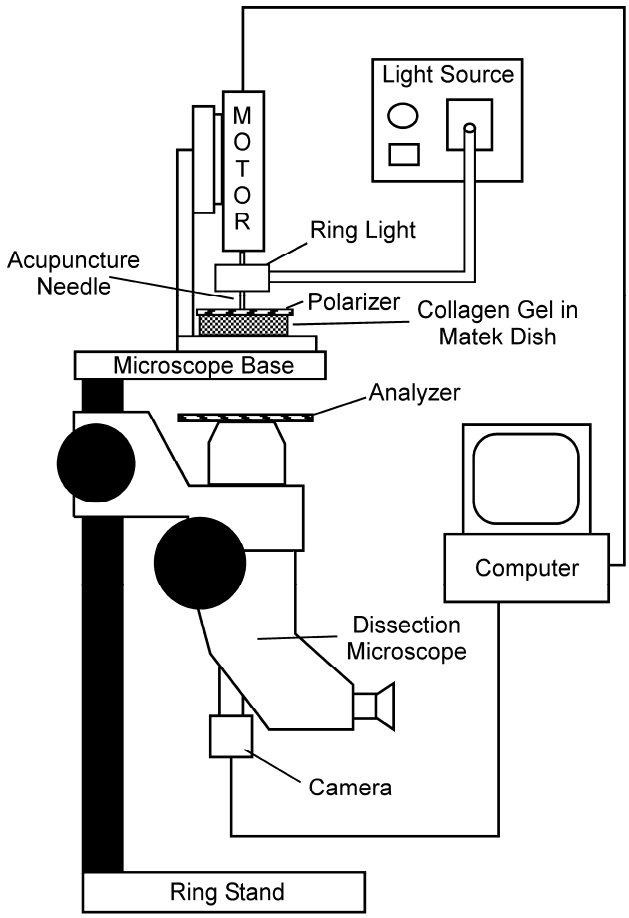

Figure 2-1: Schematic of polarized light microscopy system. A dissection stereomicroscope with a USB camera was mounted upside-down to a bench top. A fiber-optic ring light was attached to the motor housing providing a light source to the sample without hindrance from the motor. The polarizer was placed on top of the sample dish, and the analyzer was placed on the microscope as shown with the axis of polarization orthogonal to the axis for the polarizer. A small hole in the polarizer allowed free insertion and rotation of the acupuncture needle in the sample.

2.3.5 Image analysis

In all cases, PLM generated images with a '4-leaf clover' morphology of birefringence that emerged and increased in area with increasing needle rotation, extending beyond the field of the captured image, until gel failure, at which point the intensity decreased (Figure 2-2). The PLM images were imported into MATLAB to quantify the birefringence. First, the failure point for each individual experiment was identified by plotting the number of pixels with intensity greater than a given threshold value, determined as described below, against the number of needle revolutions and identifying the global maximum of the curve (Figure 2-2F). This point was confirmed by visual inspection of the image sequence. Failure points were compared statistically using a two-way ANOVA, with collagen concentration and crosslinking as fixed effects (SPSS 12.0, Chicago, IL). Significance levels were set at $P < 0.05$. The earliest failure point (rounded down to the nearest integer) among all experiments was 4 revolutions for untreated samples and 2 revolutions for crosslinked samples.

The evolution of birefringence with needle rotation, reflecting the increase in fiber alignment, was quantified by determining a continuous index of the area of alignment. To apply a consistent criterion for comparing alignment across different conditions, the image sequence for each experiment was first normalized by subtracting the mode intensity value of the first image, which was taken prior to needle rotation and represented the background intensity level, from all remaining images in the sequence. This removed background differences among different collagen concentrations and smoothed out minor day-to-day fluctuations.

To determine the operating threshold intensity for each experimental set of images, the image at 2 (crosslinked samples) or 4 (untreated samples) revolutions was binarized at decreasing threshold intensity levels, beginning with the maximum intensity present in the image. As the threshold value decreased, the binarized image began to resemble a 4-leaf clover. The operating threshold value was identified as the maximum value for which a complete clover structure was observed (Figure 2-3). Using this threshold value, each frame in the image set was converted to a binary image, and the area of pixels greater than or equal to that intensity was calculated. Comparisons among untreated collagen gels were made up to 4 revolutions, and comparisons among crosslinked collagen gels, or between crosslinked and untreated gels, were made up to 2 revolutions, the earliest failure points observed among all experiments within these respective conditions.

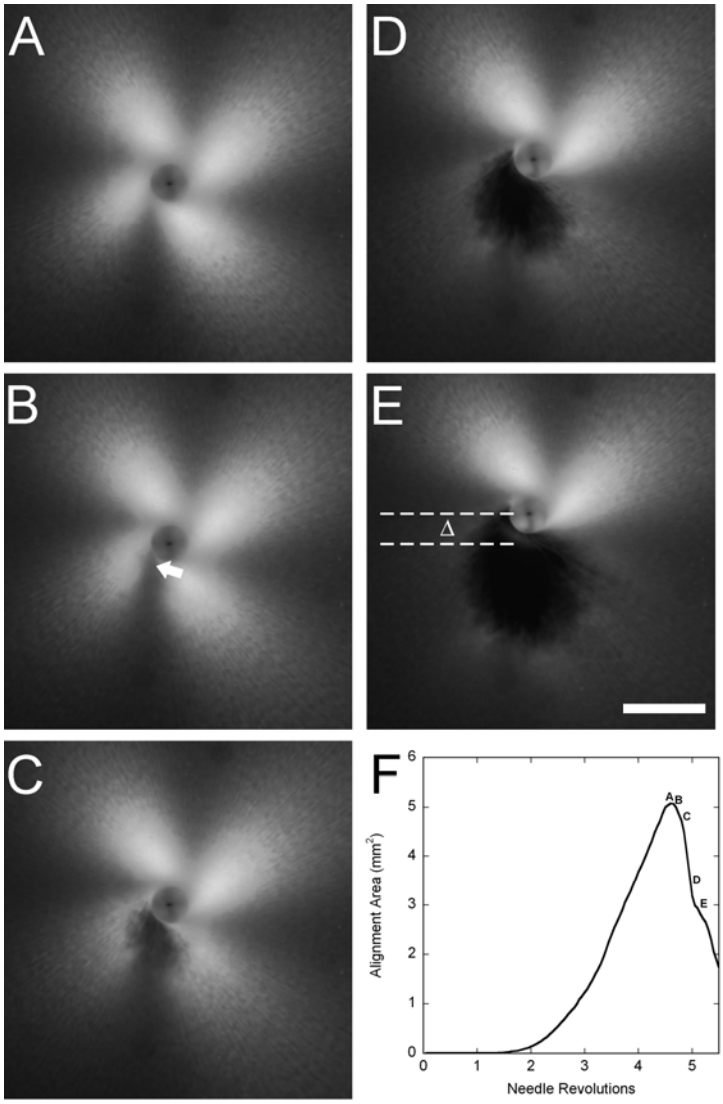

Figure 2-2: Winding and failure of collagen gels during in vitro acupuncture. (A) PLM image of the gel immediately before the onset of tearing. The characteristic '4-leaf clover' pattern of birefringence increases in size up to the point of failure as the gel becomes increasingly aligned due to winding around the needle. (B-E) Development of gel failure at 0.5sec (0.15rev) intervals. At the onset of tearing (B), a weakening of the birefringence can be observed near the needle where the dense, circumferentially wound center transitions to radially aligned fibers (arrow). As failure ensues, a hole is observed in the gel (C-E), and the residual stress in the remainder of the gel is enough to bend the needle, as indicated by the shift in needle position, Δ, directed away from the tear. The increasing size of the tear results in a decreasing area of birefringence. (F) Images A-E marked on a plot of the area above a threshold intensity vs. needle revolutions. The peak represents the image taken at maximum alignment immediately prior to the onset of failure. Bar: 1 mm.

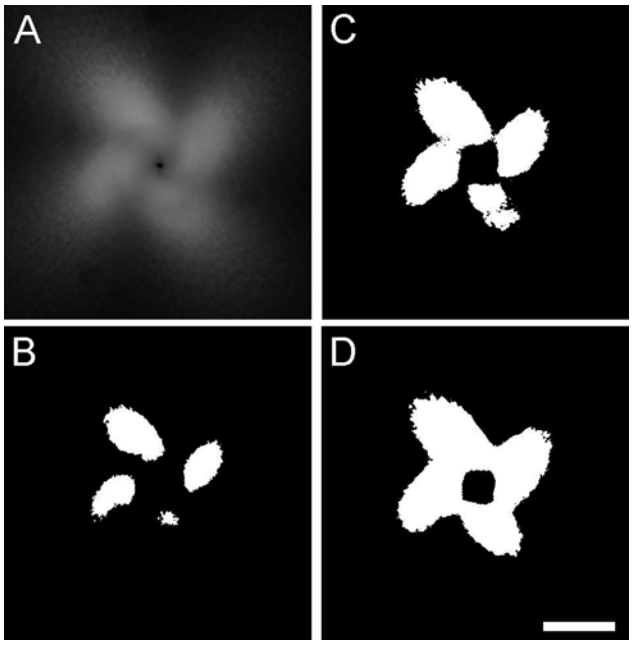

Figure 2-3: Methodology for identifying threshold criteria. From each image set, the image at 2 or 4 revolutions was extracted (A) and sequentially binarized with a decreasing grayscale value, beginning with the maximum intensity present in the image. As the threshold value decreased, the binarized image began to resemble a 4-leaf clover (B, C). The threshold value for the gel was set as the maximum grayscale value that produced a complete clover structure with no interruptions in the 4 leaves (D). Bar: 1 mm.

2.3.6 Collagen gel rheology

Parallel plate rheometry was used to assess the mechanical properties of the collagen gels. Mechanical testing was done using a Rheometrics SR-2000 parallel plate rheometer with a temperature-controlled incubation chamber maintained at 37°C (TA Instruments, New Castle, DE). A sample well was formed by punching a 25mm diameter hole in a 4mm thick layer of PDMS. Type I collagen solutions were prepared at concentrations of 1.5, 2.0, and 2.5 mg/ml, as described above, and 2ml were pipetted into the well, which was then transferred to a 37°C incubator. After self assembly, the gels were carefully removed with a spatula and transferred to the bottom plate of the rheometer. The top plate was lowered to a height of 2.0mm. The dynamic storage and loss moduli of the gels were evaluated at 1% shear strain amplitude at frequencies ranging from 0.1 – 10Hz. Five samples were tested for each of the 6 conditions. The moduli were analyzed statistically with a two-way ANOVA. Significance levels were set at $P < 0.05$.

2.4 Results

2.4.1 General observations

During continuous needle rotation, all gels exhibited tearing prior to 10 revolutions. Whereas collagen concentration did not affect the failure of the gels ($P = 0.274$), crosslinked gels failed at a significantly lower number of revolutions than untreated gels ($P < 0.001$) (two-way ANOVA) (Figure 2-4). Therefore, to compare different conditions, quantitative analyses were performed up to a standardized number of revolutions that represented the lowest integer number before failure among all samples.

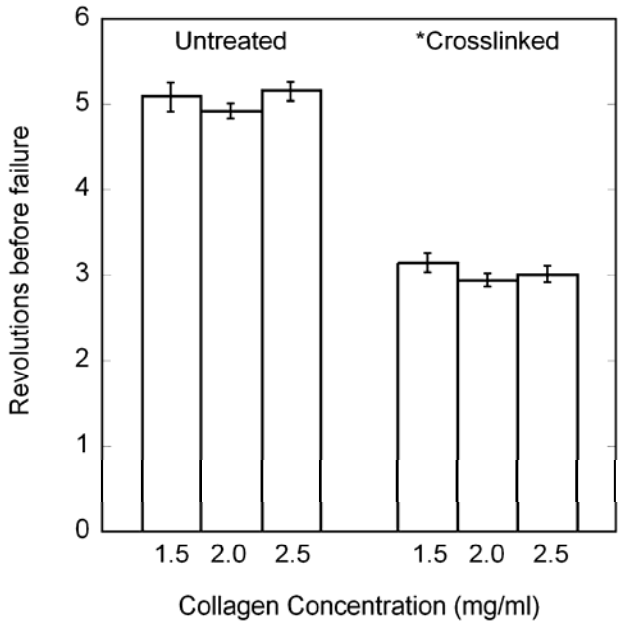

Figure 2-4: Revolutions to failure (average +/- standard error) during in vitro acupuncture. The number of revolutions before gel tearing was identified from alignment area curves and verified visually from the image sets. Crosslinking the collagen significantly decreased the ability of the collagen gels to withstand needle rotation without tearing (*, 2-way ANOVA, $P < 0.001$), whereas changing the collagen concentration had no effect ($P = 0.274$)

2.4.2 Collagen imaging

Gel morphology before and after 2 revolutions is shown in brightfield (Figure 2-5A & B), PLM (Figure 2-5C & D), and confocal (Figure 2-5E & F) images. Collagen fiber winding was not obvious in bright field images, but could be inferred from PLM images (see below), and was directly observed in confocal images. Prior to needle rotation, collagen fibers were randomly oriented. After needle rotation, circumferential alignment was observed close to the needle, which evolved into radial alignment as the distance from the needle increased (Figure 2-5F). The effect was similar but more pronounced after 4 revolutions (data not shown).

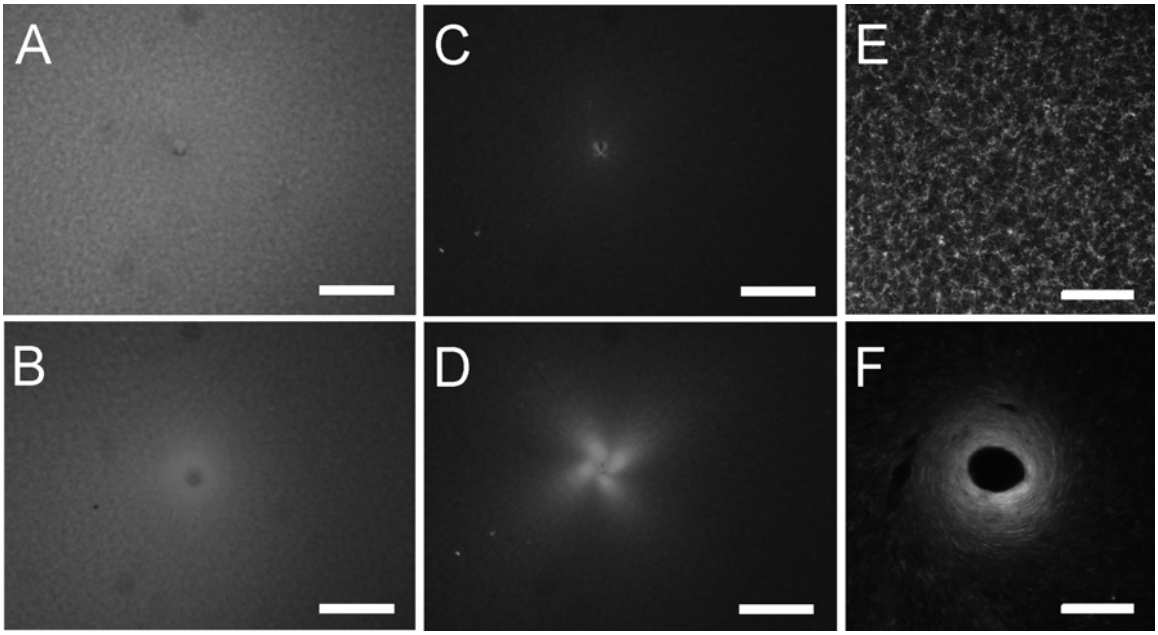

Figure 2-5: Images of 2 mg/ml fluorescently spiked collagen gels before needling and after 2 revolutions. (A) Brightfield imaging of the gel with needle inserted before needling shows a small hole in an otherwise uniform field. (B) After needle rotation, the collagen fiber density appears to change around the needle, and a faint radial pattern is observed. (C) Under cross-polars, the needle hole is again evident in an otherwise random field before needle rotation. (D) After rotation, the significant bright regions indicating collagen fiber alignment 45° off-axis. (E) Using confocal microscopy, the random orientation of collagen fibers is apparent. (F) After needling, the fiber density increases around the needle. Fibers near the needle are aligned circumferentially and transition to radial alignment away from the needle. Bars: A-D, 1mm; E-F, 50μm.

2.4.3 Quantitative PLM

The alignment pattern observed with confocal microscopy was evident in PLM images as a clover-leaf pattern of birefringence, where fiber alignment 45° off-axis generates an intensity peak. The area of alignment at the same number of revolutions was visually greater with increasing collagen concentration and in untreated collagen gels vs. crosslinked gels (up to 2 revolutions) (Figure 2-6). A continuous index of the area of alignment was generated by binarizing the complete set of images in each run using a threshold intensity as described above. For untreated collagen gels, the average area of

alignment increased more rapidly and to a higher final value with increasing concentration (Figure 2-7). Crosslinked samples aligned more gradually than untreated gels (Figure 2-8), and also demonstrated the trend of increased area of alignment with increasing collagen concentration.

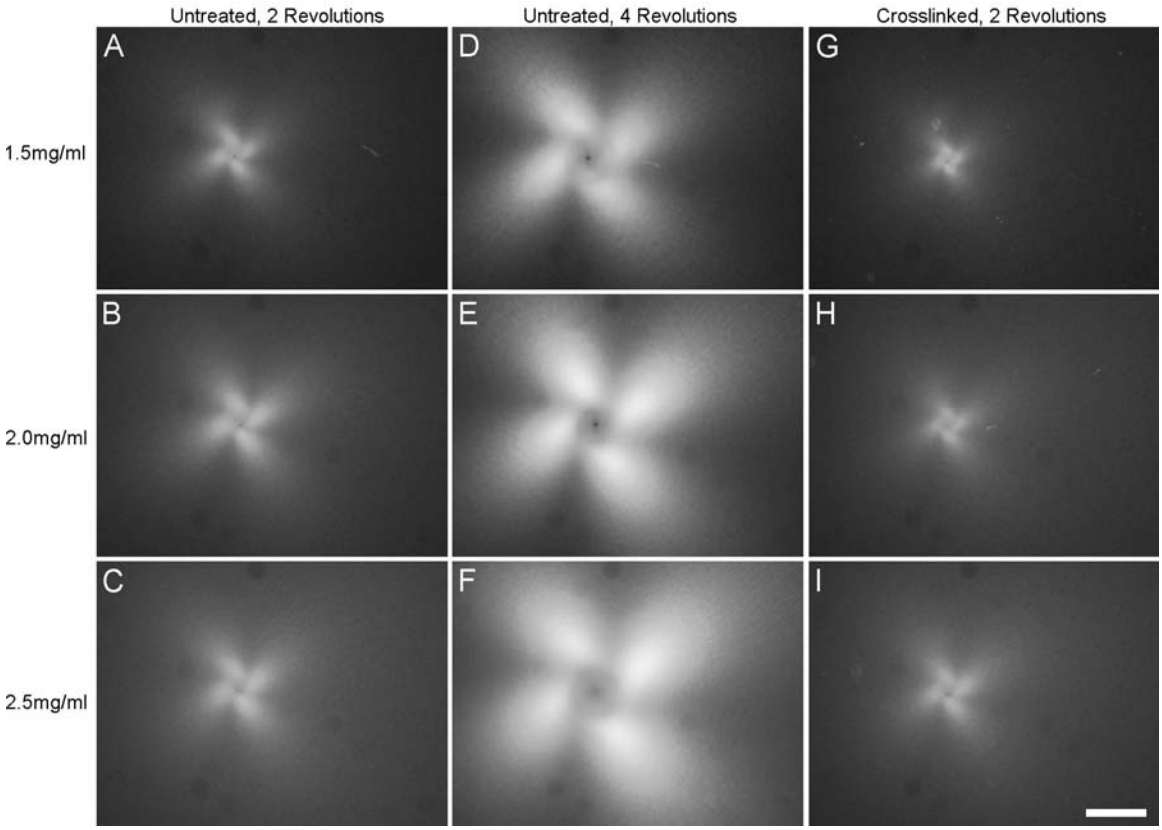

Figure 2-6. Polarized light images of collagen gel response to in vitro acupuncture after 2 needle revolutions (A-C), and 4 revolutions (D-F) in untreated collagen gels and 2 revolutions (G-I) in crosslinked gels. The birefringent area increased with increasing revolutions, and was greater in untreated collagen compared to crosslinked collagen at the same number of revolutions. This area also increased with increasing collagen concentration for each condition (A, D, G – 1.5mg/ml; B, E, H – 2.0mg/ml; C, F, I – 2.5mg/ml). Bar = 1 mm.

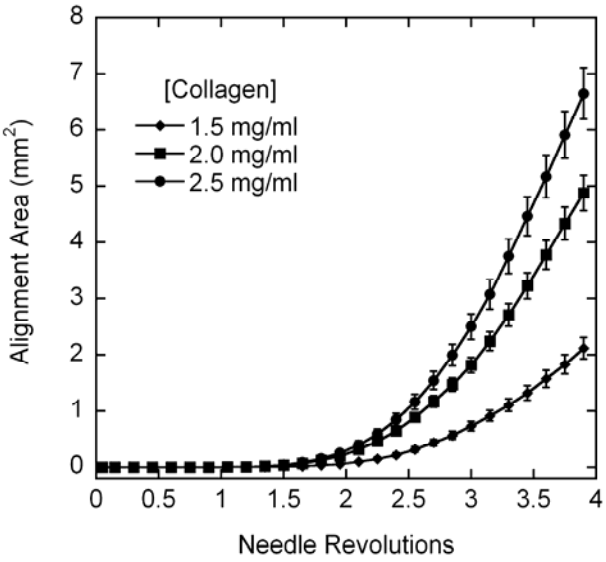

Figure 2-7: Effects of collagen concentration on area of alignment (average +/- standard error). The birefringent area of alignment was identified from image sets binarized based on the image at 4 revolutions, and plotted as a function of needle revolution. Increasing the collagen concentration increased the area.

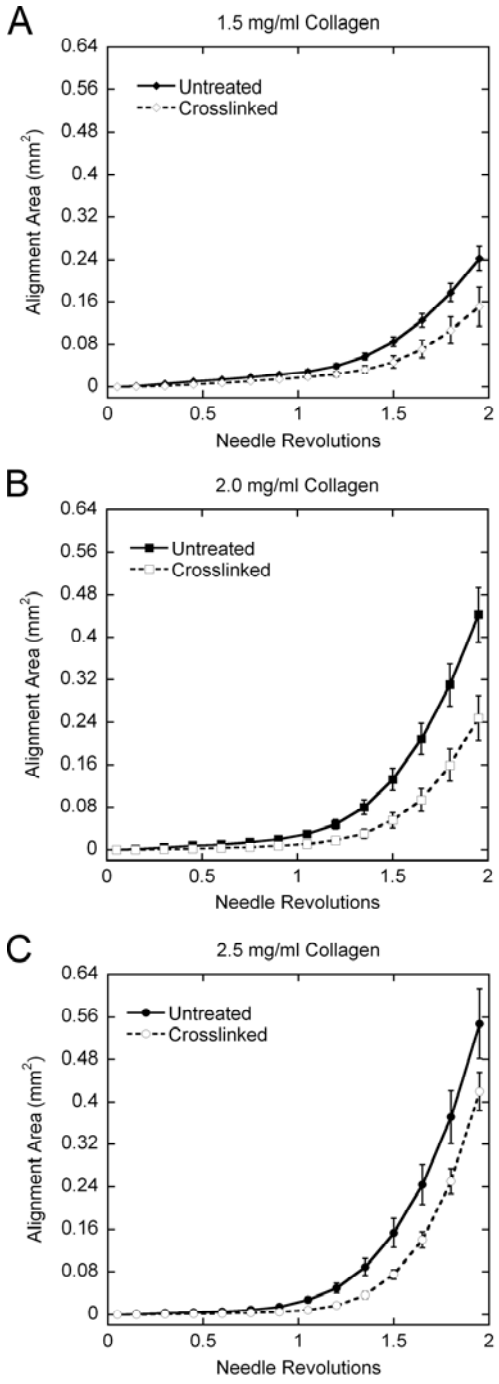

Figure 2-8: Effects of crosslinking on area of alignment (average +/- standard error). The birefringent area of alignment was identified from image sets binarized based on the image at 2 revolutions. Needle rotation in crosslinked collagen gels generated less alignment than untreated collagen gels at each collagen concentration. The area of alignment increased with increasing collagen concentration for both untreated and crosslinked collagen.

2.4.4 Depth of needle insertion

The depth of insertion study was performed with a new shipment of collagen, and preliminary experiments with collagen from the crosslinking and collagen concentration studies indicated that the new batch presented significantly less alignment than the old batch, but that trends in the response were the same. As such, experiments in the depth of insertion studies were performed exclusively with the new batch of collagen and analyzed separately from the crosslinking and collagen concentration studies. Changing the depth of needle insertion significantly affected the failure of the gels (Figure 2-9). Thicker gels failed at fewer revolutions than thinner gels. For 4mm-thick gels, increasing the depth/percentage of needle insertion decreased the revolutions before failure, but this was not observed consistently with the 6mm-thick gels. The alignment of gels was also affected by insertion depth and percentage (Figure 2-10). In vitro acupuncture with needles inserted the same depth in gels of different thickness generated more alignment in thinner gels, indicating that the fraction of the gel that is subjected to needle rotation is an important parameter in dictating the response. Maintaining the same percentage of insertion at gels of different thickness produced greater alignment in thicker gels than thinner gels. For example, inserting a needle 3mm into a 4mm-thick gel and rotating the needle produced more alignment than the same procedure in a 6mm-thick gel (inverted triangles, Figure 2-10A and B). However, inserting a needle 75% into a 6mm-thick gel (squares, Figure 2-10B) produces more alignment than 75% into a 4mm gel (inverted triangles, Figure 2-10A).

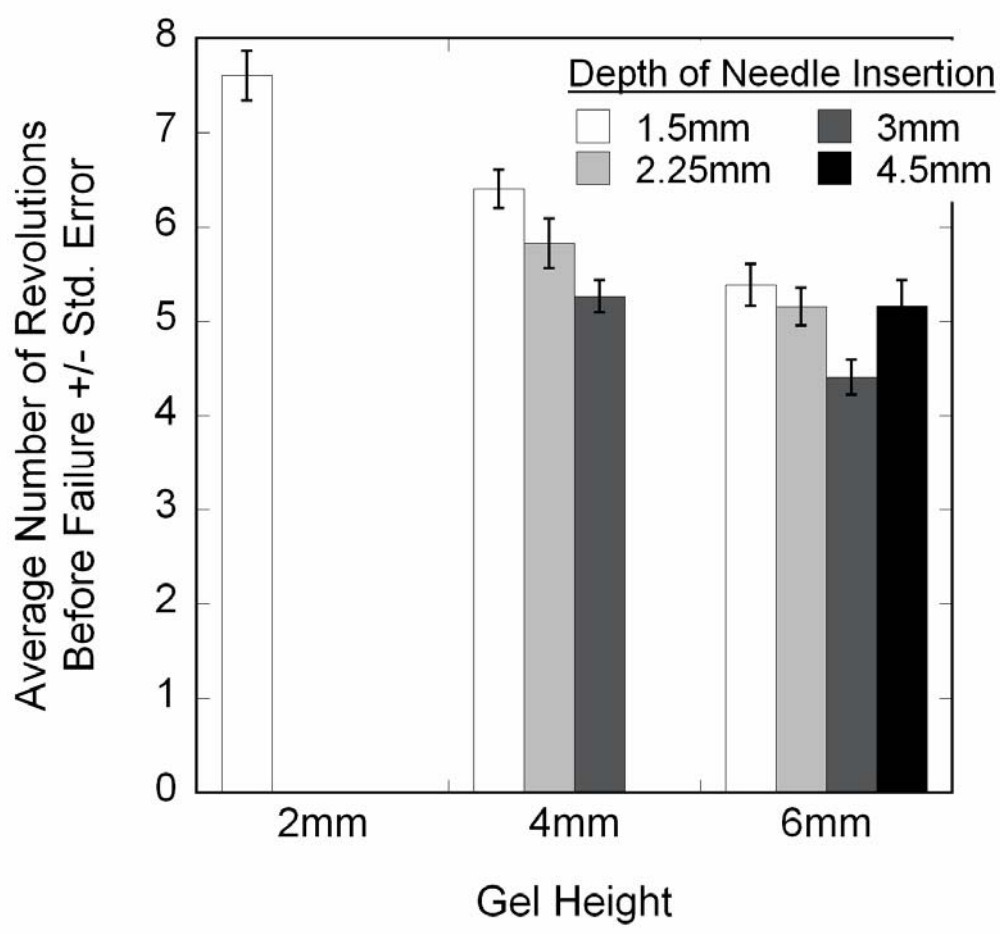

Figure 2-9: Effects of gel height and depth of needle insertion on revolutions to failure during in vitro acupuncture. Thin gels were able to withstand significantly more needling than thick ones ($P<0.001$). For 4mm-thick gels, revolutions to failure decreased as the depth of needle insertion increased, by this was not observed for 6mm-thick gels.

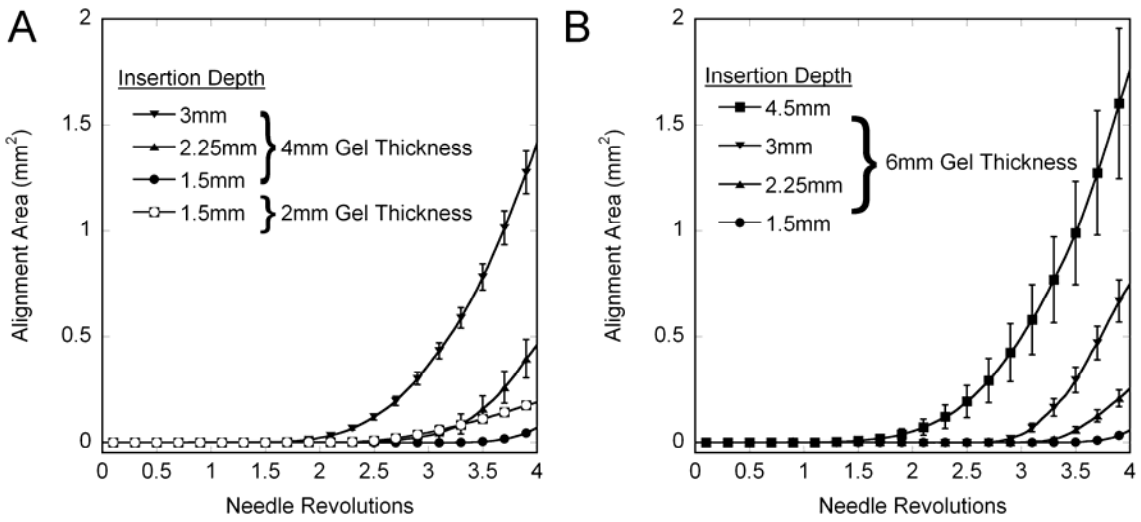

Figure 2-10: Effects of gel thickness and depth of needle insertion on the measured area of fiber alignment (average +/- std. error). A) 2mm-thick and 4mm-thick gels; B) 6mm-thick gels. For the same depth of insertion, thin gels demonstrated more alignment than thick gels. For both 4mm- and 6mm-thick gels, the alignment area increased as depth of insertion increased.

2.4.5 Rheology measurements

Storage and loss moduli were determined using parallel plate rheometry. The storage modulus showed a gradual increase with increasing frequency, before sharply dropping (Figure 2-11A). Inspection of gels revealed damage to the samples, which did not occur if experiments were run only at lower frequencies (data not shown), and we assumed that the damage was responsible for the apparent decrease in stiffness. In general, increased collagen concentration and crosslinking delayed this damage. The loss modulus for untreated gels showed a gradual increase at low frequencies, particularly for untreated collagen (Figure 2-11B). The loss modulus for crosslinked collagen decreased at moderate frequencies, and increased more sharply for all cases concurrent with the decrease in storage modulus. Two-way ANOVA revealed significant increases in the

storage and loss moduli at all frequencies with increasing collagen concentration and crosslinking (all $P < 0.001$).

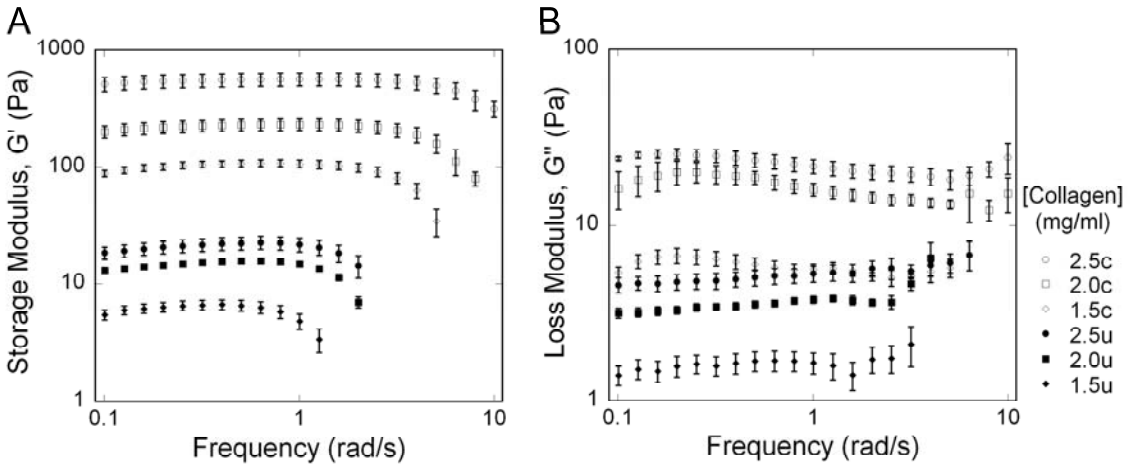

Figure 2-11: Frequency sweep of collagen gels under 1% controlled strain (average +/- standard error). A) Storage Modulus; B) Loss Modulus. Both the storage and loss moduli demonstrated significant increases with increasing collagen concentration and crosslinking (2-way ANOVA, $P < 0.001$). Key: c: crosslinked, u: untreated.

2.5 Discussion

During treatment, acupuncture therapists aim to achieve "needle grasp" as a sensory marker of an appropriate degree of needle manipulation. Recent studies suggest that needle grasp occurs when collagen fibers in the subcutaneous connective tissue attach to and wind around the needle, thus imposing a local stress and strain field on the surrounding tissue [6]. In this paper, we imaged a simple, in vitro, acellular collagen gel system using polarized light microscopy during acupuncture needle rotation and measured the degree of winding in terms of fiber alignment to identify relationships between collagen concentration, crosslinking, and winding, as well as the failure of the gels.

We found that both collagen concentration and crosslinking influenced the response to controlled acupuncture needle rotation. Alignment increased with increasing collagen concentration, but decreased in gels that were crosslinked with formalin. Crosslinked gels also failed at a significantly lower number of needle rotations than untreated gels. Failure consistently occurred ~0.25mm-1.0mm away from the needle, and corresponded to the point where circumferential alignment of collagen fibers wound around the needle transitioned to radial alignment from fibers in the periphery of the gel being pulled into the needled area. The acute change in fiber geometry likely introduced a stress concentration that ultimately caused a tear in the collagen gel.

Altering the collagen concentration increases fiber density, which has potential indirect and direct consequences on the polarized light microscopy. First, the increase in fiber density could affect the mechanical properties simply by increasing the number of structural elements to carry load and/or by increasing fiber-fiber interactions, which would affect the tissue response to needle rotation. The increase in fiber density would also influence the degree of alignment, as measured with polarized light microscopy. An increase in fiber density implies that a greater number of fibers would be aligned for the same number of revolutions, and could therefore more efficiently rotate the polarization state of the incident light.

Crosslinking the gel decreases the flexibility of individual and aggregate fibers, which had a marked effect on the mechanical properties of the gels, increasing the storage modulus in shear by about an order of magnitude. The increased rigidity of crosslinked

fibers increased the resistance to winding and deformation, and also increased the stress generated with winding, thereby leading to less alignment and earlier failure compared to untreated gels of the same concentration.

In addition to altering the mechanical properties of the gels, changing collagen concentration and crosslinking the gels could have influenced interactions and adhesion with the needle and/or the polystyrene dish. However, no gels failed at either the needle interface or the dish interface, and we believe that differences in adhesion among conditions played a minimal role in the bulk of the observed temporal response, except, perhaps, for the initial lag period in the alignment curves that represents initiation of alignment.

The differences between the response of untreated and crosslinked collagen gels to in vitro acupuncture, and particularly the earlier failure of crosslinked gels, suggests that mechanostructural differences in the soft tissues that contact an acupuncture needle during therapy may be responsible for the selective coupling and winding of collagen fibers in specific soft tissue layers during needle rotation. In vivo and explant studies have demonstrated that, although an acupuncture needle is inserted through the epidermis and dermis and into subcutaneous fat and muscle, only the subcutaneous loose connective tissue appears to specifically wind around the needle [3]. The resulting recruitment of loose connective tissue fibers towards the needle can thicken that layer and subsequently compress the overlying and underlying tissue layers, but the characteristic whorl pattern is only seen in the loose connective tissue.

The tissue properties that govern this selective adherence and winding are not yet known. However, a recent study by Iatridis et al. documented the mechanical properties in uniaxial tension of loose connective tissue from mouse explants, and noted important distinctions between loose connective tissue and other load bearing soft tissues, including skin [16]. Most soft tissues demonstrate significant non-linear stiffening above a certain strain – typically between 1% and 20%. For example, skin has a low strain modulus on the same order as loose connective tissue (2.75kPa) up to about 10% strain [17], after which the modulus increases to ~240kPa [17, 18]. In contrast, loose connective tissue demonstrated a highly linear elastic response up to 50% strain [16]. Thus, as tissue begins to wind around the needle and deform, significantly greater stress will be generated in skin vs. loose connective tissue, and, similar to the response of our crosslinked gels, we would expect the failure stress to be reached at a lower number of revolutions. The network of collagen fibers in the dermis may be too stiff to effectively respond to acupuncture needle rotation.

In clinical acupuncture, the thickness of the connective tissue layer varies, often with the thickness of subcutaneous fat, and it is especially thick at intermuscular cleavage planes. These planes correlate anatomically to acupuncture points and meridians[14], and Langevin has shown that the resistant force to needle rotation at acupuncture points is greater than at control points, where the connective tissue layer is thinner. It was suggested that needling in locations where connective tissue is more pronounced enhances the mechanical response of fibroblasts residing within this tissue [1]. In investigating how the depth of needle insertion and gel thickness may affect the response

of a homogeneous tissue, we found that both the relative depth as well as the absolute depth of insertion into the collagen gel were important factors in the failure and alignment responses. Thinner gels were able to withstand more needle rotations than thick ones. Interestingly, the failure point was reached earlier as the depth of insertion was increased in 4mm-thick gels, but no real trend was observed in 6mm-thick gels. For both 4mm-thick and 6mm-thick gels, more alignment was recorded when the depth of insertion was greater. The last observation is consistent with an increase in the number of fibers subjected to rotation via contact with the needle. We also observed that more alignment was generated for the same depth of insertion in thin gels versus thick ones. The greatest amount of alignment was observed with the greatest absolute coverage of the needle by the collagen gel – 4.5mm insertion into a 6mm-thick gel. We believe that the increase in thickness of collagen below the needle increases the physical resistance to drawing individual fibers up and in towards the needle, thereby creating more stress to stimulate resident cells. We also note that the tip of the acupuncture needle is tapered. The length of the tapered tip represents a greater proportion of the inserted needle at shallower insertion depths than deeper insertions. The biomechanical response of the gel, particularly the initial adhesion of the collagen fibers to the needle, may be influenced by needle diameter [14], which would be embedded in our needle depth results.

The differences with collagen concentration and crosslinking, as well as the empirical differences in alignment from separate batches of collagen (compare 2.0mg/ml plot in Figure 2-6 to 3mm insertion into 4mm-thick gels in Figure 2-10A), suggest that subtle changes in tissue composition and structure may affect the biomechanical response to

needle rotation in vivo, and potentially the efficacy of acupuncture therapy. It is well known that the collagen content of human skin throughout the body is non-uniform [9], and the matrix components of skin can be crosslinked, degraded, and or damaged by any number of environmental factors, including exposure to ultraviolet light, disease states, such as glycation associated with type 1 diabetes mellitus [19], and normal physiological processes, such as wound healing. There have been relatively few studies of loose connective tissue of any kind, though it is likely that the biophysical properties of this tissue also vary among individuals and with location in one individual, and may dictate, in part the efficacy of acupuncture in a particular patient or at a particular location.

It is important to keep in mind that the in vitro system developed in this work is only a first step and differs significantly from the loose connective tissue involved in acupuncture, a cellular tissue comprising primarily fibroblasts embedded in an extracellular matrix of collagen and elastin fibers and proteoglycans. We chose to begin with an acellular collagen gel, representing the most significant structural component of the extracellular matrix, to establish a baseline for further study before proceeding to the more complex cellular system, in which a number of variables can change dynamically due to fibroblast-mediated compaction, matrix synthesis, and degradation. We also chose a rotational velocity (0.3rev/sec) significantly slower than typically applied clinically to facilitate image acquisition and reduce viscoelastic effects.

2.6 Conclusion

The in vitro model provides a platform to study mechanotransduction during acupuncture in a highly controlled and quantitative setting. The results indicate that the mechanostructural properties of soft connective tissues may affect their response to acupuncture therapy. Based on the results of this work, the biofidelity of our in vitro system can now be systematically improved by introducing cells and additional matrix components, such as elastin and proteoglycans, to better mimic features of loose connective tissue, and by applying needle rotation protocols consistent with clinical practice. The incorporation of additional instrumentation to record the resistive torque that develops in the gel during needle manipulation and the strain within the gel would also significantly improve our ability to study the biomechanics associated with acupuncture. It is likely that the torque and strain, which may be transmitted to resident cells in vivo and in cellular assays in vitro to initiate mechanotransduction, are strongly influenced by gel or tissue composition as well as the rate and number of needle rotations. The system can then be used to aid in the determination of the quantitative biological response to biomechanical signals introduced during acupuncture needling.

2.7 References

1. Langevin HM, Churchill DL, Fox JR, Badger GJ, Garra BS, Krag MH: **Biomechanical response to acupuncture needling in humans.** *J Appl Physiol* 2001, **91:**2471-2478.
2. Langevin HM, Churchill DL, Cipolla MJ: **Mechanical signaling through connective tissue: a mechanism for the therapeutic effect of acupuncture.** *Faseb J* 2001, **15:**2275-2282.
3. Langevin HM, Churchill DL, Wu J, Badger GJ, Yandow JA, Fox JR, Krag MH: **Evidence of connective tissue involvement in acupuncture.** *Faseb J* 2002, **16:**872-874.
4. Langevin HM, Konofagou EE, Badger GJ, Churchill DL, Fox JR, Ophir J, Garra BS: **Tissue displacements during acupuncture using ultrasound elastography techniques.** *Ultrasound Med Biol* 2004, **30:**1173-1183.
5. Langevin HM, Bouffard NA, Badger GJ, Churchill DL, Howe AK: **Subcutaneous tissue fibroblast cytoskeletal remodeling induced by acupuncture: evidence for a mechanotransduction-based mechanism.** *J Cell Physiol* 2006, **207:**767-774.
6. Langevin HM, Bouffard NA, Churchill DL, Badger GJ: **Connective tissue fibroblast response to acupuncture: dose-dependent effect of bidirectional needle rotation.** *J Altern Complement Med* 2007, **13:**355-360.
7. Da Silva D, Vidal B, Zezell D, Zorn T, Nunez S, Ribeiro M: **Collagen birefringence in skin repair in response to red polarized-laser therapy.** *Journal of Biomedical Optics* 2006, **11:**024002-024001-024006.
8. Pierce M, Strasswimmer J, Park B, Cense B, de Boer J: **Birefringence measurements in human skin using polarization-sensitive optical coherence tomography.** *Journal of Biomedical Optics* 2004, **9:**287-291.
9. Vitellaro-Zuccarello L, Cappelletti S, Dal Pozzo Rossi V, Sari-Gorla M: **Stereological analysis of collagen and elastic fibers in the normal human dermis: variability with age, sex, and body region.** *The Anatomical Record* 1994, **238:**153-162.
10. Debessa C, Maifrino L, de Souza R: **Age related changes of the collagen network of the human heart.** *Mechanisms of Ageing and Development* 2001, **122:**1049-1058.
11. Mays P, McAnulty R, Campa J, Laurent G: **Age-related Alterations in Collagen and Total Protein Metabolism Determined in Cultured Rat Dermal Fibroblasts: Age-related Trends Parallel those Observed in Rat Skin In Vivo.** *Int J Biochem Cell Biol* 1995, **27:**937-945.
12. Vogel H: **Influence of maturation and aging on mechanical and biochemical properties of connective tissue in rats.** *Mechanisms of Ageing and Development* 1980, **14:**283-292.
13. Takahashi M, Hoshino H, Kushida K, Inoue T: **Direct Measurement of Crosslinks, Pyridinoline, Deoxypyridinoline, and Pentosidine, in the Hydrolysate of Tissues Using Hign-Performance Liquid Chromatrography.** *Analytical Biochemistry* 1995, **232:**158-162.
14. Langevin HM, Yandow JA: **Relationship of acupuncture points and meridians to connective tissue planes.** *Anat Rec* 2002, **269:**257-265.

15. Shreiber D, Enever P, Tranquillo R: **Effects of PDGF-BB on rat dermal fibroblast behavior in mechanically stressed and unstressed collagen and fibrin gels.** *Experimental Cell Research* 2001, **266:**155-166.
16. Iatridis JC, Wu J, Yandow JA, Langevin HM: **Subcutaneous tissue mechanical behavior is linear and viscoelastic under uniaxial tension.** *Connect Tissue Res* 2003, **44:**208-217.
17. Eshel H, Lanir Y: **Effects of strain level and proteoglycan depletion on preconditioning and viscoelastic responses of rat dorsal skin.** *Ann Biomed Eng* 2001, **29:**164-172.
18. Oxlund H, Manschot J, Viidik A: **The role of elastin in the mechanical properties of skin.** *J Biomech* 1988, **21:**213-218.
19. Vishwanath V, Frank K, Elmets C, Dauchot P, Monnier V: **Glycation of skin collagen in type I diabetes mellitus. Correlation with long-term complications.** *Diabetes* 1986, **35:**916-921.

CHAPTER 3: VARYING ASSAY GEOMETRY TO EMULATE CONNECTIVE TISSUE PLANES IN AN IN VITRO MODEL OF ACUPUNCTURE

3.1 Abstract

Traditional acupuncture is performed by inserting and rotating fine needles at specific points, which causes loose fascial tissue to wind around the needle. This coupling is stronger at acupuncture points, which tend to fall above intermuscular fascial planes, than control points, which lay above skeletal muscle. As such, the anatomical organization of tissues at acupuncture points presents different boundary constraints that may affect the mechanical coupling. Fascia at acupuncture points is bounded on two sides by skeletal muscle. Conversely, tissue at control points is essentially unbounded. These differences were approximated in simple in vitro models. Type 1 collagen gels were cast in circular gels of different radii to emulate the narrower boundary within the intermuscular plane, as well as elliptical gels with major and minor axes matching the large and small circular gels, respectively, and planar gels constrained on only two sides to model the anisotropic boundary conditions presented within these planes. Acupuncture needles were inserted into the gels and rotated via a computer-controlled motor at 0.3 rev/sec while capturing the evolution of fiber alignment under cross-polarization. Small circular gels aligned faster, but failed earlier than large circular gels. Needle rotation in elliptical and planar gels generated more alignment per revolution than circular gels. Planar gels were particularly resistant to failure. Alignment in circular gels was isotropic, but alignment in elliptical and planar gels was stronger in the direction of the minor axis. When fibroblasts were included in the gels, they followed the alignment of the collagen fibers, and also became denser in regions of stronger fiber alignment. These results suggest that the

anatomical organization of soft tissues at acupuncture points may provide unique boundary conditions that accentuate the mechanical response to needle manipulation.

3.2 Introduction

Although acupuncture has been clinically proven in treating conditions such as pain, nausea and hypertension [1] and has been increasingly used by patients seeking alternative medical therapies [2], the mechanisms that underlay the therapeutic benefits remain unknown. During treatment, fine needles are inserted and rotated at specific locations on the body known as acupuncture points based on the maps passed down for centuries. Manipulating these acupuncture points is believed to regulate the flow of energy or 'qi' through acupuncture meridians to produce local effects and specific, far-reaching results. Despite the evidence for clinical or functional efficacy, there is little correlation of acupuncture points and meridians to neuroanatomical or physiological structures.

Clinically, practitioners locate acupuncture points by identifying a nearby anatomical landmark, such as a bony prominence, muscle, or tendon, and then using light palpation to precisely determine the position [3]. Recently, Langevin and Yandow identified a high correlation between inter- and intramuscular connective tissue cleavage planes and acupuncture points (~80%) and meridians (~50%) by mapping acupuncture points on a cadaver to serial gross sections from the Visible Human Project (Fig 3-1) [3]. At these points, there is an abundance of loose, interstitial, connective tissue and no underlying skeletal muscle. After locating the points, practitioners insert and manipulate the needles

until they feel 'needle grasp' – described as a "fish biting on a line" – at which time the patient senses 'de qi.' Using an instrumented needling apparatus, Langevin showed that this grasping force at acupuncture points was significantly greater than control points, which did no lay above connective tissue planes. Separate work with full thickness rat abdominal wall explants, where acupuncture needles were inserted through epidermis, dermis, subcutaneous connective tissue and fat, and subcutaneous muscle and then rotated, demonstrated that only the loose, subcutaneous connective tissue wound around needle to evoke a grasping force [4]. Working with explants of just subcutaneous connective tissue, Langevin also showed that fibroblasts residing several millimeters away respond to the mechanical perturbation produced by acupuncture needle rotation with distinct morphological and cytoskeletal changes [5].

Taken together, these results suggest that mechanical forces may contribute to the cellular and tissue changes leading to therapeutic benefits following acupuncture, and. that the anatomical organization of soft tissues strongly influences the biomechanical response. However, untangling the contributions of these and other factors to the biophysical responses of tissues and cells in clinical settings or in explant studies, which present complex tissue environments, is difficult. We have developed a 3D in vitro approach to examine the biophysical and, ultimately, the cellular responses to acupuncture in a controlled setting. Using type I collagen gels as tissue mimics, we demonstrated previously that the winding response of fibrillar collagen to needle rotation resembles that of loose connective tissue and varies with network density and stiffness and the depth on needle insertion [6].

In this study, we used this in vitro approach to study the influence of the geometry of fascial planes on fiber winding. In vivo, the tissue in these planes is bounded on two sides by skeletal muscle, and generally becomes narrower with increasing depth, presenting distinct boundary conditions compared to locations above a muscle, which resembles an infinite plane (Fig 3-1) [3]. We prepared circular gels of different radii to emulate the narrower boundary within the intermuscular plane, and elliptical gels and gels constrained on only two sides to model the anisotropic boundary conditions presented within these planes. We quantified the alignment response of these gels to controlled needling, and we examined cell alignment in fibroblast-populated gels.

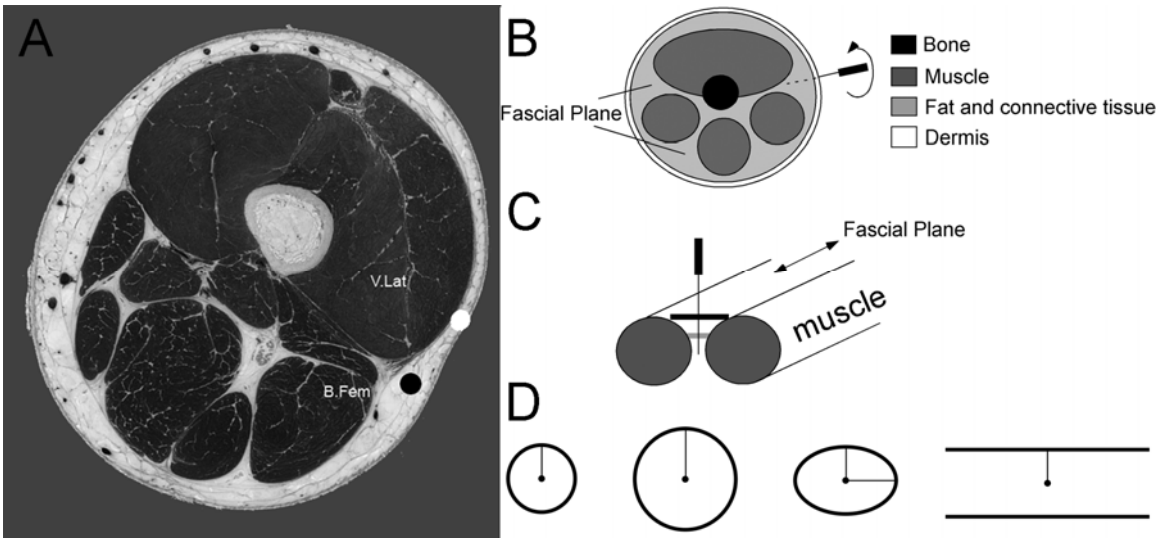

Fig 3-1: A) Anatomical section of a thigh [3]. The white dot located above the vastus lateralis (V. Lat) represents a control point. The black dot located between the V. Lat and the biceps femoris (B. Fem) above an intermuscular cleavage plane, or fascial plane, indicates an acupuncture point, and B) Simplified schematic of a cross-section of the thigh indicating different tissue types and the location of fascial planes. C) Along the axis of the muscles, the fascial plane presents a geometry that is generally bounded on two sides and narrows with increasing depth. D) Simple assays geometries emulating the basic features of the fascial planes were generated out of PPE to create geometric constraints: two circles of different diameter to examine the effects of the a narrower boundary condition, and elliptical and planar geometries to simulate the anisotropic boundary conditions where the distance to the PPE constraints is greater in one direction.

3.3 Materials and Methods

3.3.1 Collagen Gel Preparation

Collagen gel solutions were prepared from lyophilized collagen (Elastin Products, Owensville, MO) as previously described [7] to achieve a final concentration of 2.5mg/ml. The 'V' shaped geometry of a fascial plane presents two variations in geometry that affect the distance from the needle to the muscle wall, which in essence is the width of the loose connective tissue layer. These variations were emulated in vitro. First, the decrease in fascial plane width with increasing needle depth was modeled by casting collagen gels within circular hydrophilic porous polyethylene (PPE – Small Parts, Miramar, FL) annular inserts with different inner radii – 1.125" (28.6 mm) and 0.75" (19.1 mm). Second, the bounded plane, which presents a narrow width of connective tissue in one direction, was modeled by casting planar gels either between two long (~35 mm – the width of the dish), thin strips of PPE placed 0.75" apart, or within elliptical PPE inserts with major (1.125") and minor (0.75") axes matching the large and small circular inserts, respectively (Fig 3-1).

The collagen solution was poured into a 35-mm glass bottom MatTek dish with a 20-mm glass microwell (MatTek Corporation, Ashland, MA) containing the PPE inserts and incubated at 37°C for 4 hrs to ensure complete fibril formation. The imaging approach (polarized light microscopy, described below) was strongly dependent on sample thickness within the imaged region. Accordingly, the gel centerline height was maintained at 4mm for all conditions.

3.3.2 Cellular Gel Preparation

Cell populated gels were prepared using rat dermal fibroblasts (RDFs) that were isolated and expanded from neonatal transgenic rats engineered to express green fluorescent protein (GFP). RDFs were cultured in Dulbecco's Modified Eagle's Medium (DMEM; Sigma Aldrich, St Louis, MO) supplemented with 10% fetal bovine serum (FBS; Atlanta Biologicals, Lawrenceville, GA), 2 ml of 200 mM L-glutamine (Sigma Aldrich, St Louis, MO), and 2 ml of 5000 units/ml penicillin-5mg/ml streptomycin (Sigma Aldrich, St Louis, MO). Trypsinized cells were rinsed in culture medium and resuspended in a 2 mg/ml collagen solution at a cell concentration of 100,000 cells/ml.

The in vitro setup was modified slightly to enhance cell viability within the tissue equivalent constructs by suspending the gels from the PPE inserts within culture medium. The approach to create the suspended gels was not amenable to the planar gels, and cellular gels were only generated within circular or elliptical inserts. First, a poly(dimethyl siloxane) (PDMS) template was created with a 60-mm outer diameter and an inner profile matching the shape of the PPE inserts. The PDMS template was placed in a 60-mm dish, and the PPE inserts placed within the PDMS. The cell-containing collagen solution was poured into PPE ring and incubated at 37°C for 4hr. Following self assembly, the PPE inserts with attached gels were removed from the PDMS and placed in a separate 60-mm dish on short PDMS stand-offs, which introduced a small space between the bottom of the gel and the culture dish. The dish was filled with fresh culture medium, which allowed diffusive transport across both the top and bottom surfaces of the suspended gel and enhanced cell survival. After 2 days in culture, the PPE inserts and

gels were transferred to a MatTek dish and covered with medium in preparation for controlled acupuncture.

3.3.3 In vitro acupuncture

A computer controlled motor (MicroMo Electronics, Inc., Clearwater, FL) was used to needle the acellular and cellular collagen gels. For acellular gels, a 250-μm stainless steel acupuncture needle (Seirin, Tokyo, Japan) was attached to the motor and inserted perpendicular to the surface of the gel to a depth of 3mm using a calibrated micromanipulator. The needle was rotated for 10 revolutions at 0.3rev/s, during which time the evolution of fiber alignment was continuously recorded with polarized light microscopy (see below).

For cellular gels, the MatTek dish was first covered with a thin sheet of PDMS. The needle was inserted through the PDMS sheet and completely through the suspended gel. The cellular gels were needled for 2 revolutions at 0.3rev/s. After needling, the needle was detached from the motor but remained in place because of the PDMS sheet, thereby allowing the gel to be transferred to the stage of an inverted microscope for epiflourescent imaging of cell alignment without any unwinding or damage from needle removal.

3.3.4 Polarized Light Imaging

Polarization light microscopy (PLM) was used to observe and image the evolution of fiber alignment continuously in real time, as previously described [6]). A dissection

stereomicroscope (Carl Zeiss Microimaging, Thornwood, NY) with a USB camera (Matrix Vision, GmbH, Oppenweiler, Germany) was physically inverted and clamped to a benchtop, which allowed the base of the microscope to be used as a platform to hold the motor stand and MatTek dish (Fig 3-2). A fiber-optic ring light (Edmund Optics, Barrington, NJ) was attached to the motor housing. The gel was placed between two polarizers, which were positioned as 'cross-polars' with their respective angles of polarization 90° apart. In this arrangement, as the light passes through the filter-sample-filter optic train, the darkest area of the resulting image occurs where collagen fibers are oriented parallel or perpendicular to the optical axis of either polarizing element; the brightest area occurs where collagen fibers are oriented 45° to the filter's optical axis. Initially, the axes of the polarizer and analyzer were aligned with the major and minor axes of the ellipse. Images were captured at 6 frames per second during needle rotation and were analyzed with MATLAB (The Mathworks, Inc, Natick, MA), as described below. In cases where needling was stopped before gel failure, after the needle rotation was complete, samples were imaged under additional polarization states where the polarizer and analyzer were rotated to 22.5^{o} and 45^{o} off the ellipse's major axis to observe anisotropy in the alignment pattern due to the asymmetric boundaries (Fig 3-3).

PLM-generated images were imported into MATLAB (The Mathworks, Inc, Natick, MA) to quantify the birefringence using previously described methods [6]. The evolution of birefringence with needle rotation, reflecting the increase in the fiber alignment, was quantified by determining a continuous index of the alignment area using a thresholding algorithm previously described [6], where the alignment area was the area of pixels

greater than or equal to the threshold intensity. These alignment curves demonstrated a sharp decrease upon failure of the gel, which enabled determination of the number of revolutions before gel tearing.

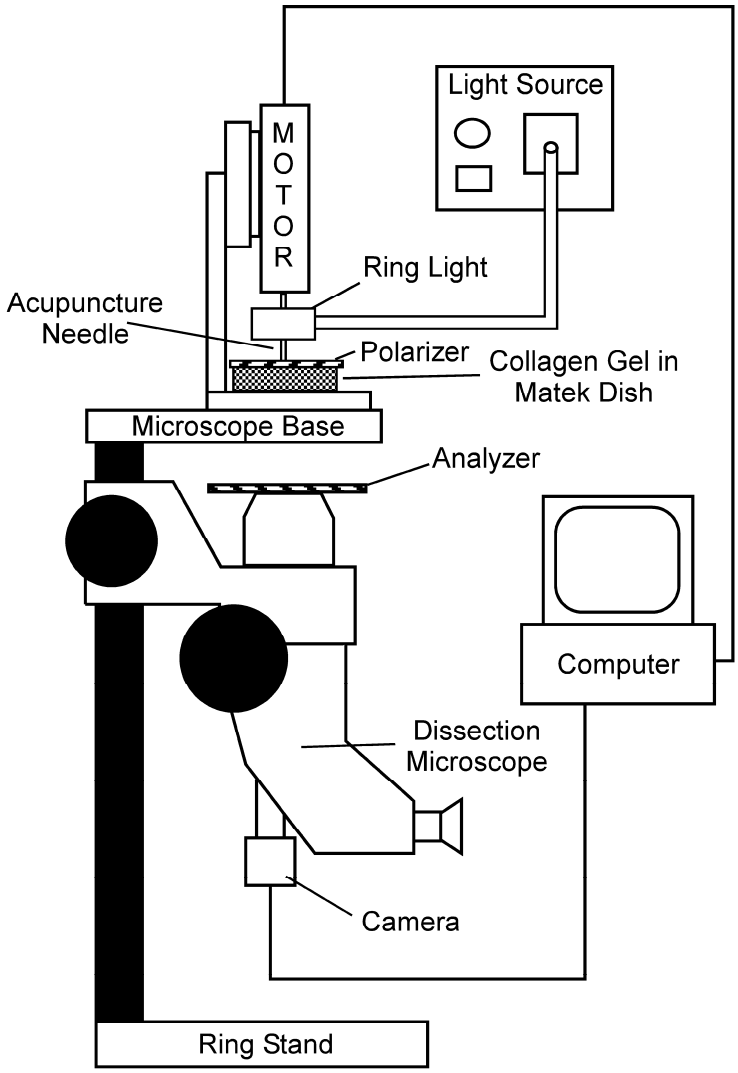

Fig 3-2: Schematic of polarized light microscopy system [6]. A dissection stereomicroscope with a USB camera was mounted upside-down to a bench top. A fiber-optic ring light was attached to the motor housing providing a light source to the sample without hindrance from the motor. The polarizer was placed on top of the sample dish, and the analyzer was placed on the microscope as shown with the axis of polarization orthogonal to the axis for the polarizer. A small hole in the polarizer allowed free insertion and rotation of the acupuncture needle in the sample.

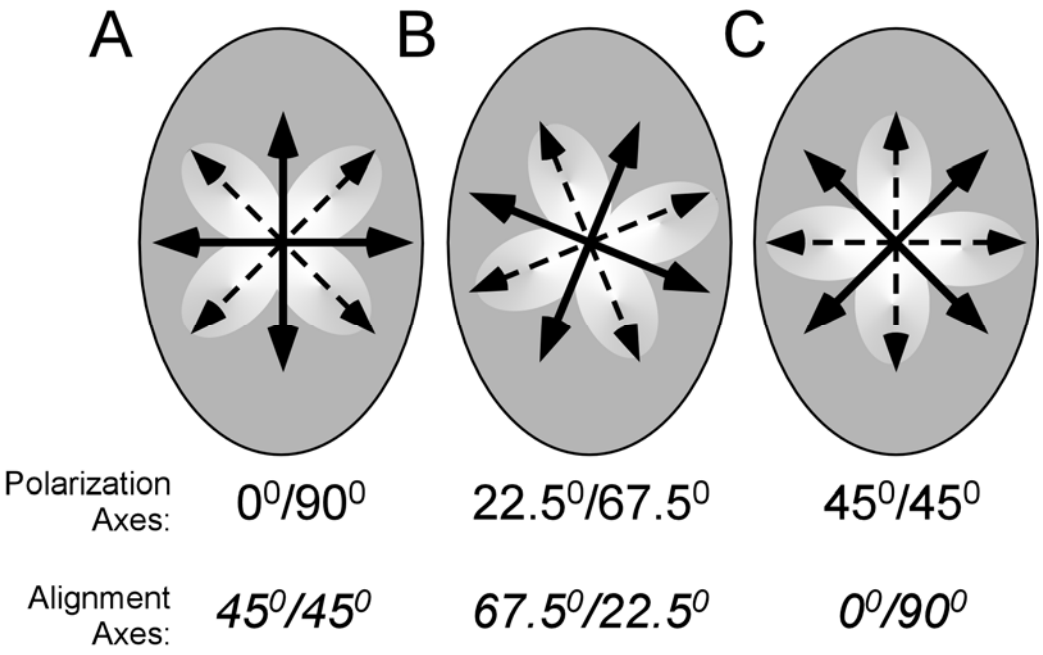

Fig 3-3: The orientation of the axes of polarization (solid lines) with respect to the major and minor axes of the elliptical assay were rotated to assess fiber alignment in different directions (dashed lines/clover leaf pattern). A) When the polarization axes are coincident with the axes of the ellipse (0°/90°), fiber alignment is evaluated at 45°, which is symmetric with respect to the ellipse. The polarization axes are rotated to be 22.5°/67.5° (B) and 45°/45° (C) off of the axes of the ellipse to examine anisotropy in alignment.

3.3.5 Cell Alignment Quantification

Cell-populated gels were imaged before and after needle rotation using an Olympus IX81 inverted microscope (Olympus, Melville, NY) using 4x magnification and FITC optics. A motorized focus was used to capture several images through the thickness of the sample. Elliptical assays were oriented with the major axis horizontal to the captured image. Cell alignment was quantified from the images by tracing the major axis of a cell and determining the projection ($\cos\theta$)of the cell-axis vector to the radial vector position of its location with respect to the needle position (Fig 3-4). These values were squared to

produce an alignment index, $\Phi = \cos^2\theta$ for each cell, where $\Phi = 1$ indicated radial alignment and $\Phi = 0$ indicated circumferential alignment [8]. Plots of Φ with respect to centroid position were created to assess the spatial distribution of cell alignment.

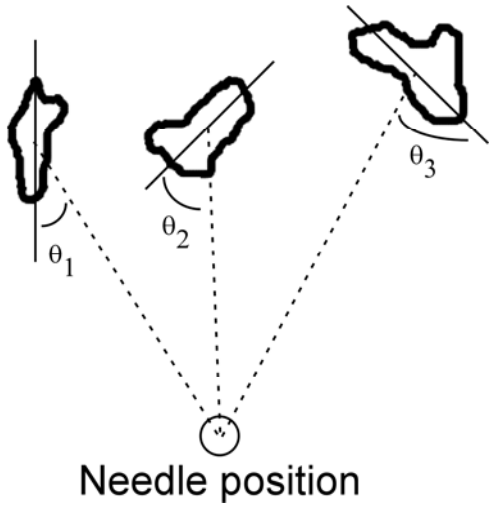

Fig 3-4: Alignment was quantified for individual cells by projecting the long axis of the cell onto a radial vector connecting the centroid of the cell to the needle position to determine cos θ. These projections were squared to create an index, $\Phi=\cos^2\theta$ ranging from 0 (circumferentially aligned) to 1 (radially aligned).

3.3.6 Statistics

Statistical comparisons were made among conditions using one-way ANOVA. When appropriate post hoc pairwise comparisons were made with Tukey's test. Significance levels were set at $P < 0.05$.

3.4 Results

3.4.1 Effects of Assay Geometry on Fiber Winding

Rotating acupuncture needles within collagen gels cast in different geometries produced alignment that presented in a form of '4-leaf clover' using PLM, which increased in area with increasing needle rotation. Differences in alignment area at 2.4 revolutions were statistically significant (ANOVA, $P < 0.001$) (Fig 3-5A). The alignment curves indicated that gels with anisotropic dimensions demonstrated more alignment than gels with uniform dimensions (Tukey's test, max $P < 0.02$), except when the planar gels were compared to the small circles ($P = 0.162$). Differences between the planar and elliptical gels were indistinguishable ($P = 0.761$). Smaller circular gels produced more alignment area than larger circular gels, though the results were not statistically significant following post hoc comparison ($P = 0.176$). Failure of the gels consistently presented as a tearing within the body of the gel, and did not occur at the interface with the needle or at the interface with the PPE wall. The smaller circular gels failed at the lowest number of revolutions, followed by the elliptical gels, the large circular gels, and finally the planar gels (ANOVA followed by pairwise comparisons with Tukey's test, max $P = 0.002$) (Fig 3-5B). The planar gels has the greatest alignment at failure ($P < 0.001$ for all pairwise comparisons); alignment at failure between the elliptical and large circular assays was statistically indistinguishable ($P = 0.768$), and alignment was least in the small circular gels ($P < 0.001$ for all pairwise comparisons) (Fig 3-5C).

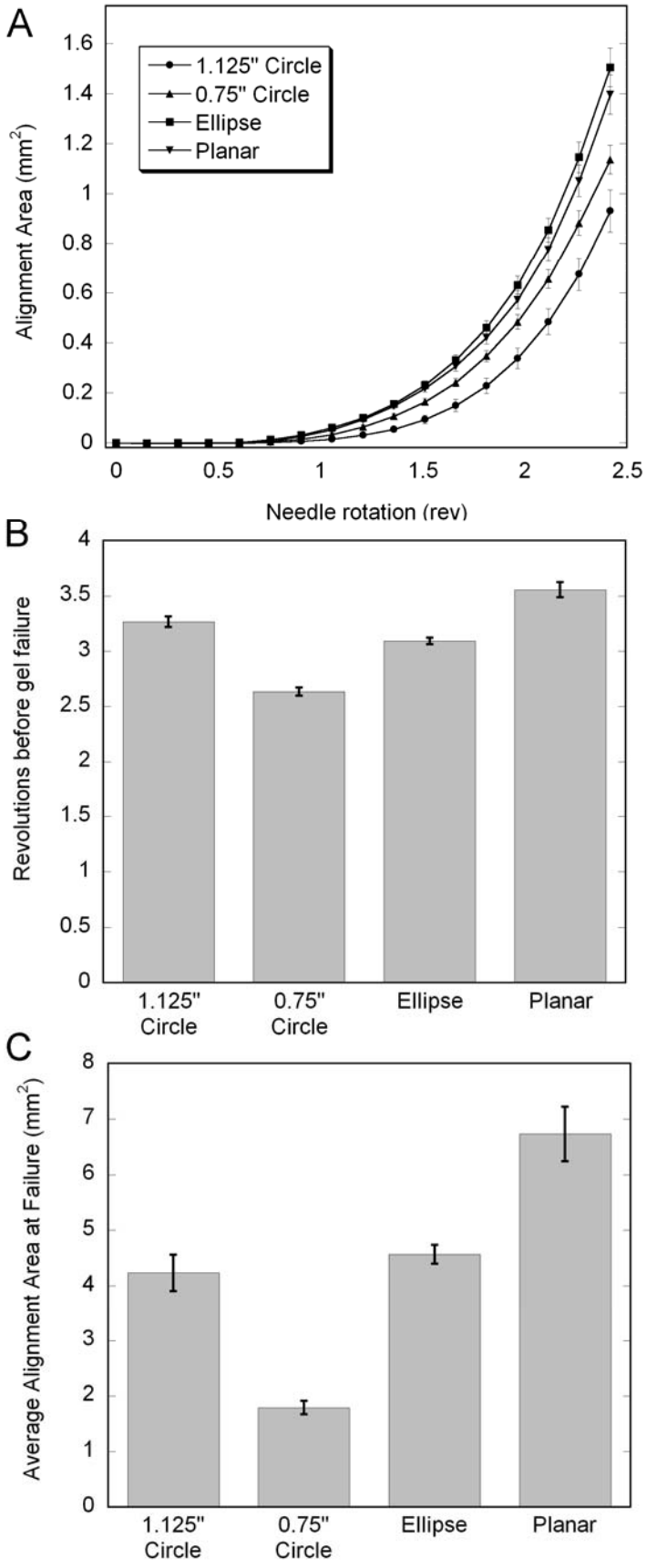
A
1.125" Circle
0.75" Circle
Ellipse
Planar
Alignment Area (mm²)
Needle rotation (rev)
B
Revolutions before gel failure
1.125" Circle
0.75" Circle
Ellipse
Planar
C
Average Alignment Area at Failure (mm²)
1.125" Circle
0.75" Circle
Ellipse
Planar

Fig 3-5: Effects of assay geometry on gel failure and fiber alignment. (A) Evolution of alignment area (average +/- standard error) up to 2.4 revolutions, which represented the fewest revolutions before failure across all conditions. (B) Average revolutions (+/- standard error) before gel failure. (C) Average alignment area (+/- standard error) at failure. Small diameter circular gels generated more alignment per revolution that larger gels, but also failed earlier, and the alignment at failure was greater for the larger gels. Introducing a non-uniform boundary condition significantly affected both alignment and failure. Fibers in the elliptical geometry aligned faster than in either circular assay but failed in between the two. The net alignment at failure was the same statistically as that produced in the large circles. When the anisotropy was increased with the planar gels, gels aligned at the same rate as in the ellipses, but were able to withstand the most number of revolutions before failure (Tukey's test, $P<0.001$), which enabled the planar gels to demonstrate the greatest alignment at failure ($P<0.001$)

3.4.2 Effects of Assay Geometry on Alignment Pattern

The initial coincident orientation of the crossed-polars with respect to the assay axes generated a PLM image of fiber alignment with a prevailing orientation of 45^{o} to the major and minor axes of the elliptical gel (or the vertical and horizontal axes of the circular gels) (Fig 3-6). For these cases, each of the 4 'clover leafs' were roughly equal in shape and size because of the symmetry of the four quadrants of alignment with respect to the geometry. By rotating the crossed-polars, alignment in other directions was assessed. The degree of anisotropy if the clover pattern was described as the ratio of the size of the leafs on perpendicular axes (Fig 3-6G). As the orientation was changed, the circular gels still presented largely uniform alignments. However, the alignment image in the planar and elliptical gels was non-uniform, with significantly stronger alignment occurring in the direction of minor axis when compared to the circular gels (max $P < 0.001$), which was consistent with a stronger alignment field in a smaller circular assay.

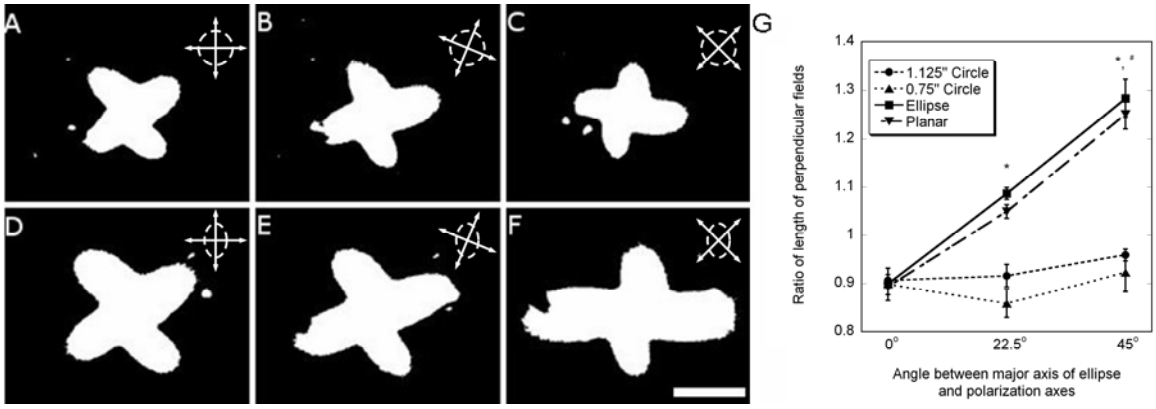

Fig 3-6: Effects of changing the orientation of the polarization axes (cross in upper right hand corner) with respect to the assay geometry (1.125" circle A-C; or ellipse D-F, shown) on the clover-leaf pattern. Within circular gels with uniform boundaries, the clover leaf patterns remained symmetric regardless of the polarization axes. Patterns within elliptical and planar gels were symmetric when the axes were coincident with the major and minor axes, but became increasingly asymmetric as the angle was changed to 22.5º (E) and 45º (F). The degree of asymmetry was expressed as the ratio of the length of perpendicular (opposite) leafs in each assay geometry (G). The elliptical and planar geometries became increasingly asymmetric as the polarization axis was rotated (* - significantly different than 0º, # - significantly different than 22.5º, ANOVA followed by Tukey's pairwise comparisons.)

3.4.3 Effects of Assay Geometry on Cell Alignment

Fibril and cell alignment in cell-populated gels was consistent with the fiber alignment observed in acellular gels. Fibril and cell alignment appeared stronger along the minor axis of the elliptical gels, but was uniform in circular gels, and in both cases extended to the boundaries of the assay (Fig 3-7). To quantify cell alignment, an alignment index, Φ was calculated for each cell in a z-stack of images and plotted at the cell centroid (Fig 3-8). Before needling, cells were randomly aligned, and the average value of Φ was close to ideal value of 0.5. After needling of circular gels, cells were primarily oriented radially, and the alignment was uniform with respect to angular position at the same radius. In elliptical gels, radial alignment occurred preferentially along the minor axis, and cells within the remainder of the gel appeared to be aligned randomly. Statistical comparison

of average alignment values demonstrated that cells in both circular and elliptical gels became significantly more aligned after needling ($P < 0.001$). Cell number also increased significantly in the needled gels ($P < 0.001$), which coincided with the substantial displacement of fibers toward the needle. Within circular gels, cell density appeared to be uniform with respect to circumferential position, but was greater along the minor axis within elliptical gels.

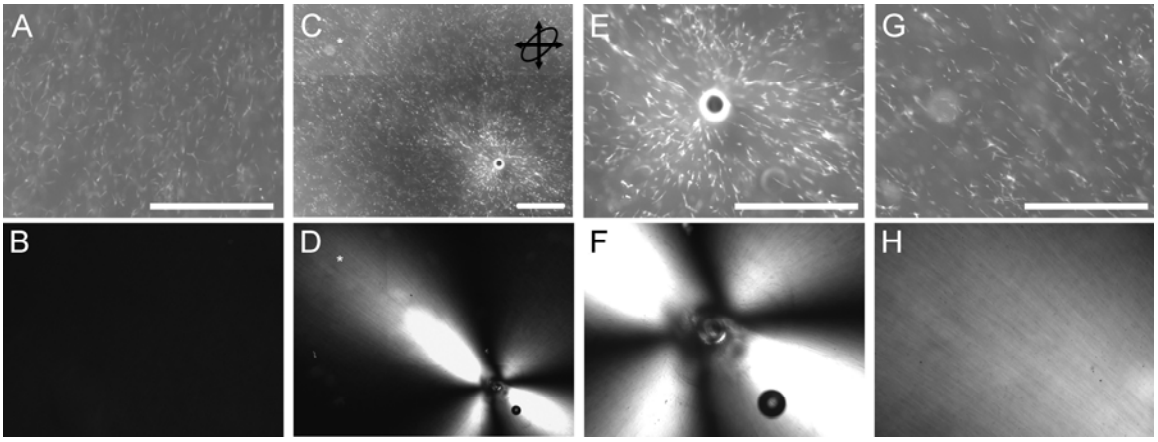

Fig 3-7. Epifluorescence images of GFP-expressing fibroblasts (top) and polarized light images of fiber orientation (bottom) in elliptical gels demonstrate that cell alignment follows fiber alignment. Before needle rotation, cells appeared randomly oriented (A), and PLM images are uniformly dark (B). After 2 needle rotations, significant alignment of cells (C) and fibers (D) is observed, particularly in the direction of the minor axis of the ellipse (shown in upper right-hand corner of (C)). A higher magnification image of cell alignment near the needle (E) demonstrates radial alignment that falls off faster in the major axis direction than the minor axis direction, which correlates to the corresponding PLM image of fiber alignment (F). The alignment is propagated along the minor axis several millimeters away from the needle (* in C & D, shown at high magnification in G & H). Bar 1mm.

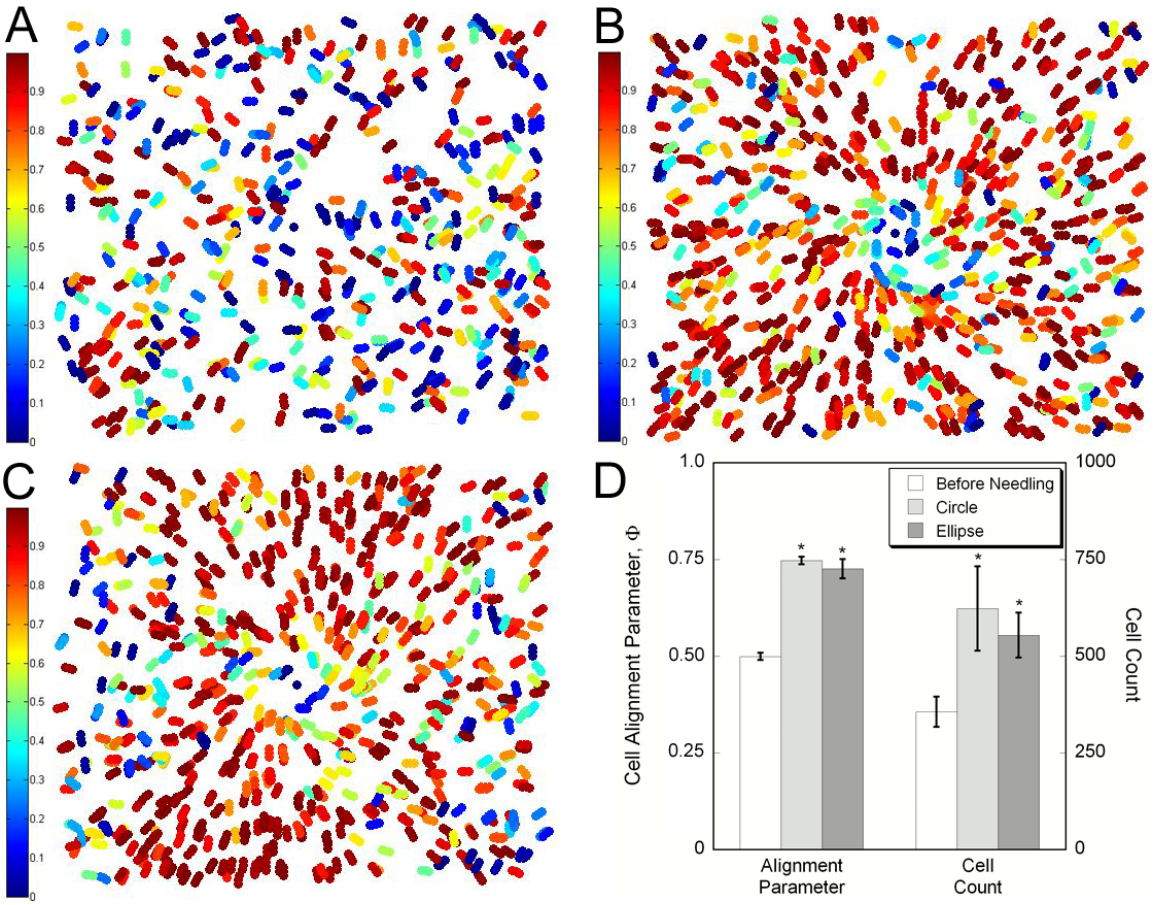

Fig 3-8: Quantitative assessment of the cell alignment parameter, Φ, which ranges from 0 (circumferential alignment – blue) to 1 (radial alignment – red). The alignment parameter was calculated for each cell in a stack of images and projected onto the same plot. Representative plots are shown for gels before needling (A), and after needling in circular (B) and elliptical (C) gels, where the major axis is oriented horizontally. Before needling, cells are randomly oriented. After needling, alignment increases in both circular and elliptical gels. Some circumferential alignment is apparent near the needle, but the prevailing orientation is radial. The radial alignment is uniform throughout the field in circular gels. In elliptical gels, radial alignment is preferentially seen in the direction of the minor axis. (D) The average alignment in the different conditions was significantly greater after needling than before needling, where Φ was approximately the predicted value of 0.5 for random alignment. The average cell count in the imaged area also increased after acupuncture needle rotation, demonstrating the significant displacement of cells and collagen towards needle as the fibers wind around the needle.

3.5 Discussion

Recent research has suggested a role for loose connective tissue located along inter- and intra-muscular fascial planes in transferring mechanical signals imparted by needle manipulation to resident cells via displacement and deformation of the tissue. In humans, in addition to increased amounts of loose connective tissue, these planes also present a distinct geometry compared to 'control' locations [3]. For the same number of needle rotations, the 'grasping' force is greater when therapy is applied at acupuncture points located above a fascial plane than control point located above skeletal muscle [9]. Using simple in vitro analogs, we demonstrated that the geometrical constraints present in the narrowing channels of connective tissue at fascial cleavage planes may act to accentuate the mechanical response of the tissue to needle manipulation.

When considering the anatomical organization of loose connective tissue (eg Fig 3-1), the tissue at control points above skeletal muscle is effectively unbounded, whereas the connective tissue at acupuncture points is bounded by muscle groups. Although not to the same disparity, we believe we captured the essence of this distinction in boundary conditions by altering the shape and size of the collagen gel. We used two metrics as indices of the mechanical response - collagen fiber alignment and gel failure. The strength of alignment – demonstrated as brighter regions in PLM– is a function of the orientation of fibers and the number/density of oriented fibers. We found that alignment was stronger when boundaries were closer to the needle, which is not surprising. It is well documented that anisotropic deformations of fibrillar materials, such as collagen gels, generates fiber alignment that is dependent on the magnitude of the disparity of

deformation in different directions [10, 11]. Needle rotation in circular gels, when the causes uniform winding of collagen fibers wind around the needle, drawing in fibers from the surrounding gel. At the perimeter, these fibers are constrained via intercalation with the PPE wall, thereby preventing circumferential movement. As a result, the fibers throughout the bulk of the gel straighten radially, and the closer the boundary is to the needle, the faster these fibers align. Since the distance to the boundary constraint is uniform around the perimeter, the alignment field is isotropic with respect to radial position. Coincident with development of the uniform alignment is an increase in stress in the system that is also uniform. Accordingly, the gels with smaller diameter fail after fewer needle revolutions.

When the boundary is non-uniform, as with the ellipse or planar gels, there is greater resistance to displacement along the minor axis or across the plane. The fibers still align radially, but also accumulate along the minor axis to become denser and generate a stronger alignment signal, thereby resulting in non-uniform alignment measurements with respect to angular position, as was demonstrated by rotating the polarization axes. The stronger alignment in the 'shorter' direction was consistent with results from the circular gels and the anisotropy predicted by simple mechanics. The allowance for displacement appeared to shield the gel from failure as well. Elliptical gels failed after a greater number of needle revolutions than the small circular gels, despite demonstrating greater alignment. Planar gels demonstrated an even greater resistance to failure, surpassing even the larger circle. As in our previous study [6], in all gels, the failure occurred within the

belly of the gel, approximately where circumferential alignment transitions to radial alignment, which places the fibers under a significant shear load.

When fibroblasts were included in the gels, the cells aligned to follow the collagen fibers, similarly to that observed in rat and mouse full thickness tissue explants [12]. Cell alignment in the circular gels was circumferential near the needle, and then became radial, and was uniform with respect to angular position. The elliptical gels also produced circumferentially aligned cells near the needle, but radial alignment was more prevalent in along the minor axis of the ellipse. Coincident with the significant increase in alignment was an increase in cell density. Despite large areas along the major axis that lacked alignment, the average cell alignment and cell number in the elliptical gels were the same as the circular gels, which also points to the relatively greater displacement of the tissue towards the minor axis in the elliptical assay than in the circular ones.

Together with our previous in vitro study, these results provide quantitative illustrations of the distinct features of loose connective that help to explain its unique capabilities to transfer mechanical load during acupuncture therapy. Specifically, the anisotropic boundaries presented within connective tissue planes appear to allow a greater volume of fibrous tissue to be displaced and deformed and shields that tissue from tearing, thereby increasing the mechanical stimulus introduced during therapy. These locations also have more of the loose connective tissue, which can further accentuate the response.

Studies by Langevin [5, 13, 14] have demonstrated that this mechanical stimulus can induce morphologic and phenotypic changes in fibroblasts, and there is a growing body of literature that substantiates the role of mechanotransduction in dictating cellular physiology and pathophysiology [15-19]. However, if these signals generated during acupuncture can be propagated along meridians, and whether the mechanical signals play a role in the therapeutic benefits, remain to be elucidated. In this study, even after only two needle revolutions, cells (and fibers) were aligned several millimeters away from the needle, and manipulations in vivo are typically more substantial [13, 20]. The results demonstrating stronger fiber alignment (and presumably mechanical signaling) in the narrower direction in our assays suggests that the signal generated by a single needle would be better propagated across a connective tissue plane rather than along the plane. However, the increase in cell and fiber density results from recruitment and displacement along the tissue plane. Moreover, these results point to the crucial role of boundary conditions in enabling fiber winding. Not every position along a connective tissue plane is recognized as an 'acupuncture point', and a more precise examination of the mechanical barriers at these locations is warranted. Furthermore, in a clinical setting, acupuncture therapy most often involves manipulation of multiple needles along a plane [21, 22], which could further introduce constraining boundaries to tissue displacement and alter the strength and direction of mechanical stimulation.

3.6 References

1. *NIH Consesus Statement on Acupuncture*. 1997, NIH.
2. Eisenberg, D., et al., *Trends in alternative medicine use in the United States, 1990-1997.* JAMA, 1998. **280**(18): p. 1569-1575.
3. Langevin, H.M. and J.A. Yandow, *Relationship of acupuncture points and meridians to connective tissue planes.* Anat Rec, 2002. **269**(6): p. 257-65.
4. Langevin, H.M., et al., *Evidence of connective tissue involvement in acupuncture.* Faseb J, 2002. **16**(8): p. 872-4.
5. Langevin, H.M., et al., *Dynamic fibroblast cytoskeletal response to subcutaneous tissue stretch ex vivo and in vivo.* Am J Physiol Cell Physiol, 2005. **288**(3): p. C747-56.
6. Julias, M., et al., *An in vitro assay of collagen fiber alignment by acupuncture needle rotation.* Biomed Eng Online, 2008. **7**: p. 19.
7. Shreiber, D., P. Enever, and R. Tranquillo, *Effects of PDGF-BB on rat dermal fibroblast behavior in mechanically stressed and unstressed collagen and fibrin gels.* Experimental Cell Research, 2001. **266**: p. 155-166.
8. Knapp, D.M., E.F. Helou, and R.T. Tranquillo, *A fibrin or collagen gel assay for tissue cell chemotaxis: assessment of fibroblast chemotaxis to GRGDSP.* Exp Cell Res, 1999. **247**(2): p. 543-53.
9. Langevin, H.M., et al., *Biomechanical response to acupuncture needling in humans.* J Appl Physiol, 2001. **91**(6): p. 2471-8.
10. Barocas, V.H. and R.T. Tranquillo, *A finite element solution for the anisotropic biphasic theory of tissue-equivalent mechanics: the effect of contact guidance on isometric cell traction measurement.* J Biomech Eng, 1997. **119**(3): p. 261-8.
11. Barocas, V.H. and R.T. Tranquillo, *An anisotropic biphasic theory of tissue-equivalent mechanics: the interplay among cell traction, fibrillar network deformation, fibril alignment, and cell contact guidance.* J Biomech Eng, 1997. **119**(2): p. 137-45.
12. Langevin, H.M., D.L. Churchill, and M.J. Cipolla, *Mechanical signaling through connective tissue: a mechanism for the therapeutic effect of acupuncture.* Faseb J, 2001. **15**(12): p. 2275-82.
13. Langevin, H.M., et al., *Subcutaneous tissue fibroblast cytoskeletal remodeling induced by acupuncture: evidence for a mechanotransduction-based mechanism.* J Cell Physiol, 2006. **207**(3): p. 767-74.
14. Langevin, H.M., et al., *Connective tissue fibroblast response to acupuncture: dose-dependent effect of bidirectional needle rotation.* J Altern Complement Med, 2007. **13**(3): p. 355-60.
15. Bride, J., et al., *Indication of fibroblast apoptosis during the maturation of disc-shaped mechanically stressed collagen lattices.* Arch Dermatol Res, 2004. **295**: p. 312-317.
16. Eshel, H. and Y. Lanir, *Effects of strain level and proteoglycan depletion on preconditioning and viscoelastic responses of rat dorsal skin.* Ann Biomed Eng, 2001. **29**(2): p. 164-72.
17. Grinnell, F., *Fibroblast biology in three-dimensional collagen matrices.* Trends in Cell Biology, 2003. **13**(5): p. 264-269.

18. Grinnell, F., et al., *Dendritic fibroblasts in three-dimensional collagen matrices.* Molecular Biology of the Cell, 2003. **14**: p. 384-395.
19. Stegemann, J. and R. Nerem, *Phenotype modulation in vascular tissue engineering using biochemical and mechanical stimulation.* Annals of Biomedical Engineering, 2003. **31**(4): p. 391-402.
20. Langevin, H.M., et al., *Tissue displacements during acupuncture using ultrasound elastography techniques.* Ultrasound Med Biol, 2004. **30**(9): p. 1173-83.
21. Eshkevari, L., *Acupuncture and pain: a review of the literature.* Aana J, 2003. **71**(5): p. 361-70.
22. Yamashita, H., et al., *Systematic review of adverse events following acupuncture: the Japanese literature.* Complement Ther Med, 2001. **9**(2): p. 98-104.

CHAPTER 4: ROLE OF TISSUE COMPOSITION ON ALIGNMENT RESPONSE

4.1 Introduction

Therapeutic acupuncture involves the insertion and manipulation of fine needles at specific points. The locations of these points dictate the therapeutic effects and are based on acupuncture maps that have been handed down for years. Although acupuncture has been commonly used [1, 2] and proven for its effectiveness in treating pain, nausea, and hypertension, the mechanisms behind acupuncture needling resulting in a remote therapeutic effect from stimulation point is yet to be elucidated. A critical first step is to identify the local changes that occur during needle manipulation, which can then be related to longer-term and more remote consequences.

In vivo and ex vivo studies have demonstrated that loose subcutaneous connective tissue couples to needles during therapeutic manipulation, which deforms the tissue. The state of stress and/or strain induces fibroblasts to alter their morphology and phenotypic behavior [3-5], and the alignment of the tissue and cells may help to propagate signals along acupuncture meridians. Although mechanical coupling occurs at both acupuncture and control points, the coupling is greater at acupuncture points [6]. For example, given the same number of rotations, more force is required to remove a needle inserted at an acupuncture point than a control point [6]. Most (~80%) acupuncture points are located at fascial planes, infolds located between muscles bundles filled with loose connective tissue [7], and the abundance of these tissues may be responsible for the increased needle coupling. Using a novel 3D in vitro model that emulates loose connective tissue in a highly controlled setting with a collagen gel, we demonstrated that rotation in thicker gels

does produce more tissue stimulation, which we measured by evaluating the alignment of the tissue. By comparing the response of collagen gels to crosslinked collagen gels, to approximate the difference in mechanical properties between loose connective tissue and dermis, we found that compliance was an important variable in dictating the ability for the tissue to withstand needle rotation without tearing. By altering the geometry of the in vitro assay, we also found that the anatomy of fascial planes may enable more needle manipulation and greater displacement of tissue. Collectively, these studies identify properties of loose connective tissue and acupuncture points that point to the unique ability for acupuncture therapy to stimulate, at least mechanically, a specific layer of tissue, and demonstrate the utility of our in vitro system for systematically examining variables of interest in a controlled yet relevant setting.

In this chapter, we further expand the model to examine the role of tissue composition on gel response. Human tissue compositions can vary not only through out the body but also from individual to individual [8], and may also vary with age, sex, race, and even as a result of a disease. Simple changes in composition can affect not only the fibrillar matrix formation but also the mechanical properties, both of which we believe will influence the response to acupuncture therapy.

To determine if different tissue compositions lead to altered mechanics during in vitro acupuncture, we prepared 2-component composite gels comprising type I collagen mixed with either hyaluronic acid (HA) or fibrin. Collagen and HA exist normally in tissues, where the amount is known to differ not only from patient to patient but also varies with age [9]. Fibrin (initially as fibrinogen, which is enzymatically cleaved by thrombin into

fibrin) is found within injured tissues and wounds that are unable to heal or heal properly, and may also be present near 'leaky' vessels that are dilated because of a local inflammatory response. Acupuncture is often applied to treat such disorders [10], and punctures the skin to cause a wound (albeit very minor) during therapy. Collagen-fibrin composite gels have been also made as tissue engineered biocompatible scaffolds [11].

4.2 Materials and Methods

4.2.1 Material Preparation

Two types of composite gels were prepared, collagen-fibrin and collagen-HA. Stock solutions were first prepared: a) 6mg/ml collagen, prepared by dissolving lyophilized collagen from bovine calf skin (Elastin Products, Owensville, MO) in 0.02N acetic acid, b) 42.5 mg/ml fibrinogen (Sigma Aldrich, St Louis, MO), prepared by dissolving fibrinogen powder in M199 (Sigma Aldrich), c) 5 unit/ml thrombin, prepared by dissolving thrombin powder in 10xMEM (Sigma Aldrich), d) 14.7 mg/ml HA, prepared by dissolving HA powder (Sigma Aldrich) in M199 and 10xMEM. The stock concentrations were chosen for easy preparation of gels with different compositions.

4.2.2 Composite Gel Preparation

4.2.2.1 Collagen-fibrin composite gels

Collagen-fibrin composite gels were prepared following the collagen gel preparation as previously described [12]. Briefly, collagen solutions were neutralized with 1N NaOH (Sigma Aldrich) and diluted to the desired final concentration using M199 and MEM containing fibrinogen and thrombin to reach final concentrations as listed in the Table 4-

1. This allowed us to examine the effects of different composite formulations at various total protein concentrations.

Calcium is necessary for thrombin to cleave fibrinogen into fibrin,and all gels, including those without fibrinogen, were supplemented with additional 0.1 mg/ml Ca^{2+}.The amount of thrombin within these gels was kept at 0.1 unit thrombin/mg fibrinogen. In all cases of collagen-fibrinogen composites, 28.6mm diameter gels were made by pouring 3ml of composite solutions into 35-mm glass bottom MatTek dishes (MatTek Corporation, Ashland, MA) containing porous polyethelyne (PPE) rings (Small Parts, Miramar, FL) and incubated at 37°C for 4hr. The solution intercalated with the pores of the PPE rings to produce a fixed boundary condition at the perimeter of the gel.

4.2.2.2 Collagen-HA composite gels

Collagen-HA composite gels were prepared using similar methods. Briefly, collagen solutions were neutralized with 1N NaOH and diluted to desired final concentration using M199 and MEM containing HA to reach final concentrations as listed in table 1, which allowed us to study the effects of HA addition within 2mg/ml collagen gels (column H-J, table 4-1). We previously made gels by pouring 3ml of composite solutions into 35-mm glass bottom MatTek dishes and incubated at 37°C for 4 hr. With PPE rings, we were able to make smaller gels, which allowed us to study effects of HA in 35mm diameter gels without PPE ring and 28.6mm diameter gels using PPE rings. The pH of composite gels was maintained between 7.2-7.4.

Table 4-1. List of gel assayed

	Total Protein	%F							%HA		
		0	20	33	50	67	80	100	0	33	50
A	2 mg/ml	2C0F			1C1F			0C2F	2C0HA		
B	2.5 mg/ml	2.5C0F	2C0.5F				0.5C2F	0C2.5F			
C	3 mg/ml	3C0F		2C1F	1.5C1.5F	1C2F		0C3F		2C1HA	
D	4 mg/ml				2C2F						2C2HA
		A	B	C	D	E	F	G	H	I	J

#C#F: '#' represents collagen (C) and fibrinogen (F) concentrations (mg/ml)
#C#HA: '#' represents collagen (C) and hyaluronic acid (HA) concentrations (mg/ml)

4.2.3 In Vitro Acupuncture

A 250-μm stainless steel acupuncture needle (Seirin, Tokyo, Japan) was attached to a computer-controlled motor (MicroMo Electronics, Inc, Clearwater, FL) and inserted perpendicular to the surface of composite gels to a depth of 3mm using a calibrated micromanipulator. The needle was rotated at 0.3rev/s for 10 revolutions.

4.2.4 Polarized Light Imaging (PLM)

The evolution of fiber alignment was continually recorded using polarized light microscopy as previously described [13]. Briefly, composite gels were placed between two polarizers, which were positioned as 'cross-polars' with their respective angles of polarization 90^o apart. With this arrangement, brightest areas occur where collagen fibers are oriented 45^o to the filter optical axis. Images were captured at 6 frames per second during needle rotation and analyzed with MATLAB (The Mathworks, Inc, Natick, MA) [13].

4.2.5 Image Analysis

PLM generated images were imported into MATLAB to quantify the birefringence using previously described methods [13]. The evolution of birefringence with needle rotation, reflecting the increase in the volume of fiber alignment, was quantified by determining a continuous index of the alignment area within an image. Images were binarized using the previously described algorithm [13], where the alignment area was the area of pixels greater than or equal to the threshold intensity. We were able to obtain the alignment area

for each sample as the alignment was developed in response to needle rotation. We also determined the number of needle revolutions at which a gel failed. The number of revolutions before failure was identified visually from image sets and verified from the curve of alignment areas.

4.2.6 Micromechanical Testing

Mechanical properties of composite gels were assessed by measuring the displacement of a small, metallic bead under a controlled magnetic force using methods previously described [14]. Briefly, a 1/32" diameter chrome-steel bead (Small Parts) was entrapped within a gel in a 0.5ml microcentrifuge tube. Images were taken to acquire the bead displacement as voltage was altered to incrementally change the applied magnetic field and generate a force-deflection curve. The force-deflection curve was then related to the elastic modulus using the following equations [14].

$$F = a(x)V^2$$

$$Slope = \frac{\mathrm{F}}{\delta}$$

$$E = \frac{F}{2\pi\delta R_o}$$

where a(x) is a calibration curve that is related to the distance between the magnet and the bead, the V is the applied voltage, δ is the bead deflection, E is the elastic modulus, and R_o is the bead diameter.

4.2.7 Statistics

Statistical comparisons were made using two-way ANOVA. Tukey's method of post hoc pairwise comparisons were used to compare within groups. Significance levels were set at $P < 0.05$.

4.3 Results

4.3.1 Collagen – Fibrin Composite Gels

4.3.1.1 Alignment

With PLM, changes in brightness surrounding the needle indicated that alignment occurred immediately after the start of needle rotation. A '4 leaf clover' was observed following needle rotation, which represented both radial and circumferential alignment (Figure 4-1). As shown in the plots (Figure 4-1M-O), regardless of composition, alignment increased with increasing total protein concentration (ANOVA, $P<0.001$). Both PLM generated images and plotted curves showed that when total protein concentration was held constant, alignment was increased with the relative fraction of collagen (Figures 4-1 and 4-2). Gels with increased collagen content tended to generate alignment faster than increased those with fibrin content.

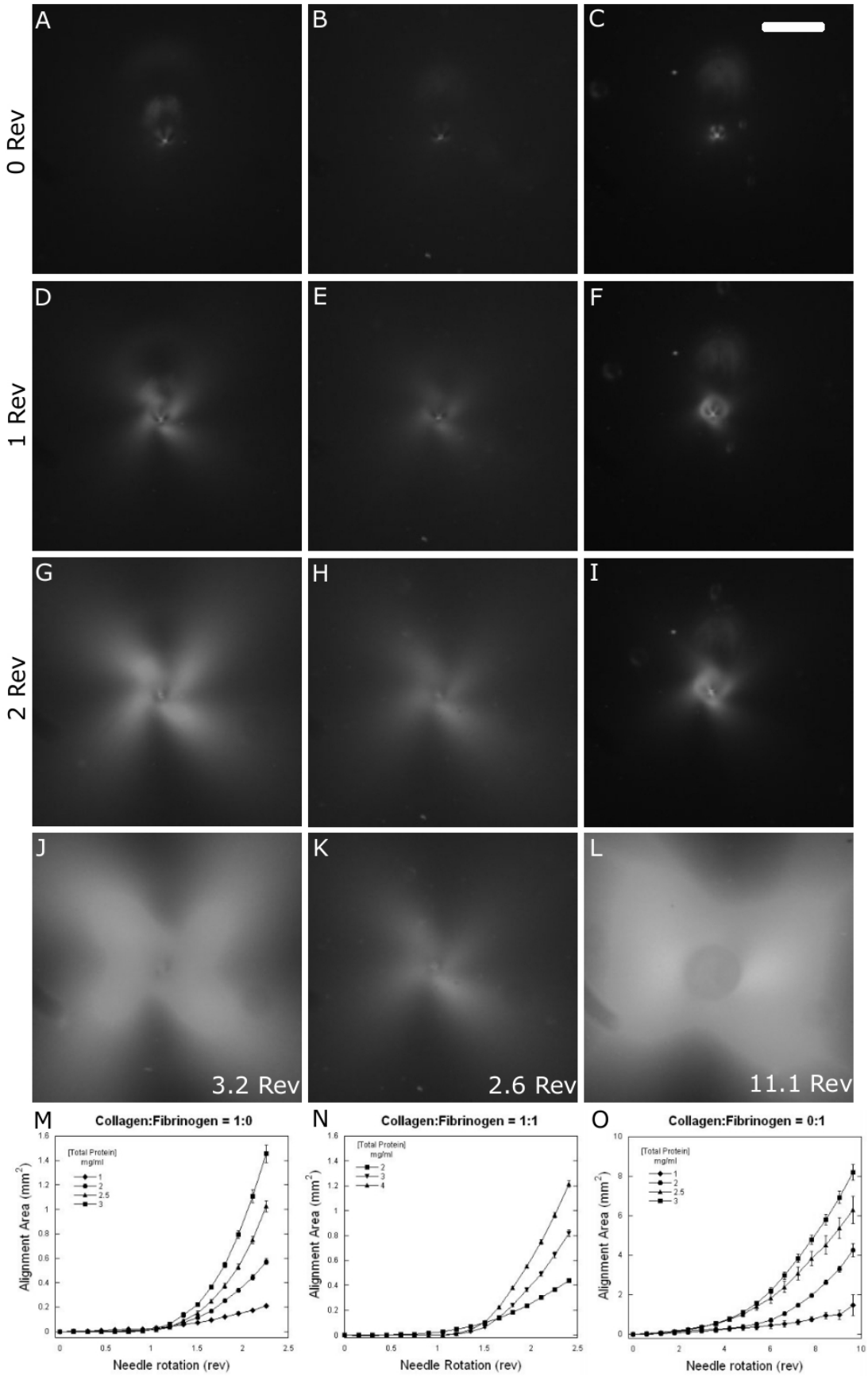
A
B
C
0 Rev
D
E
F
1 Rev
G
H
I
2 Rev
J
K
L
3.2 Rev
2.6 Rev
11.1 Rev
M
Collagen:Fibrinogen = 1:0
[Total Protein] mg/ml
1
2
2.5
3
Alignment Area (mm^2)
Needle rotation (rev)
N
Collagen:Fibrinogen = 1:1
[Total Protein] mg/ml
2
3
4
Alignment Area (mm^2)
Needle Rotation (rev)
O
Collagen:Fibrinogen = 0:1
[Total Protein] mg/ml
1
2
2.5
3
Alignment Area (mm^2)
Needle rotation (rev)

Figure 4-1. Representative polarized light images (A-L) of gel response to acupuncture in vitro within 0%F gels (column I), 50%F gels (column II), and 100%F gels (column III) with 3 mg/ml total protein content, where the alignment was increased with number of needle rotations. The birefringent area was greater in lower fibrinogen content gel at the same number of revolutions. Images at gel failure (J-L) showed 100%F gels were able to reach higher alignment than 0%F gels by withstanding further needle rotations. Bar = 1 mm. The plots (M-O) indicated alignment was increased with total protein concentration.

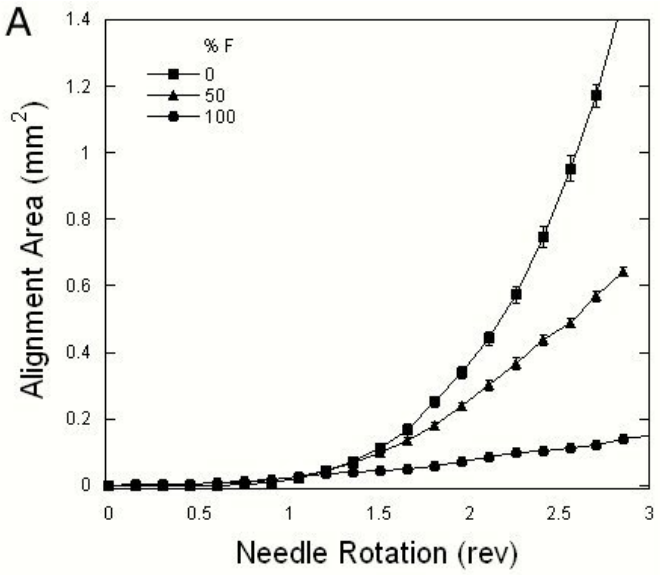
A
% F
0
50
100
Alignment Area (mm2)
Needle Rotation (rev)
0
0.2
0.4
0.6
0.8
1
1.2
1.4
0.5
1.5
2
2.5
3

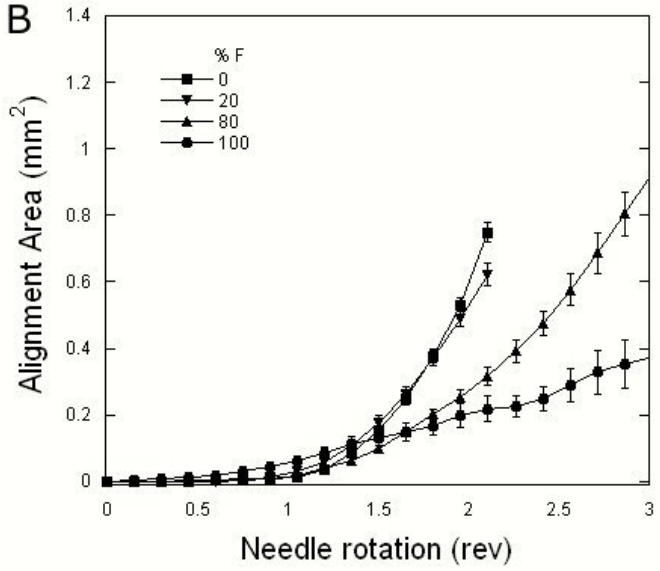
B
% F
0
20
80
100
Alignment Area (mm2)
Needle rotation (rev)
0
0.2
0.4
0.6
0.8
1
1.2
1.4
0.5
1.5
2
2.5
3

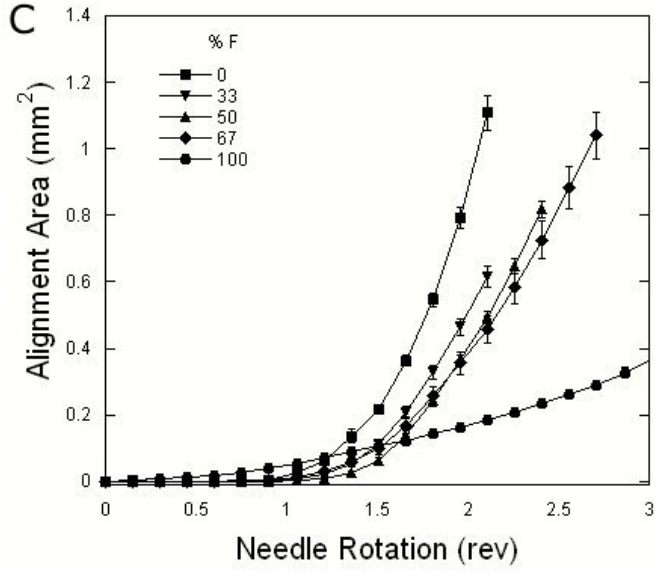
C
% F
0
33
50
67
100
Alignment Area (mm2)
Needle Rotation (rev)
0
0.2
0.4
0.6
0.8
1
1.2
1.4
0.5
1.5
2
2.5
3

Figure 4-2. Effects of gel composition on the alignment area (average +/- standard error). The birefringent area of an alignment was identified from image sets binarized based on the image at 2 revolutions, and plotted as a function of needle revolution. Composition effects were observed within total protein of 2.0mg/ml (A) 2.5mg/ml gels (B) and 3.0mg/ml gels (C). At the same total protein content, the alignment was found decreasing with increasing fibrinogen content. Uneven curve lengths were mainly because gels with different compositions failed at different number of needle rotations. F: fibrinogen.

4.3.1.2 Gel failure

Failure consistently occurred within the gel body, and there was no failure or gel detachment at the needle interface or at PPE wall boundaries. Similar to previous findings, changing protein concentrations within pure collagen gels had no effect on gel failure. Protein concentration was a significant factor ($P=0.028$) for pure fibrin gels, but there were no discernible trends shown with pairwise comparisons (Figure 4-3a). In general, fibrin gels failed at later number of needle rotations than collagen gels (ANOVA, $P<0.001$). There is no significant difference in gel failure when compare within composite groups, except in gels with relatively high fibrinogen content (>80%F), which were able to sustain more than double the number of rotations compare to gels with high relatively high collagen content (Tukey's, $P<0.001$).

Since alignment tended to increase non-linearly with needle rotations, gels that failed earlier had lower alignment at failure, whereas gels that were able to withstand more number of needle rotations would have relatively higher alignment (Figure 4-3b).

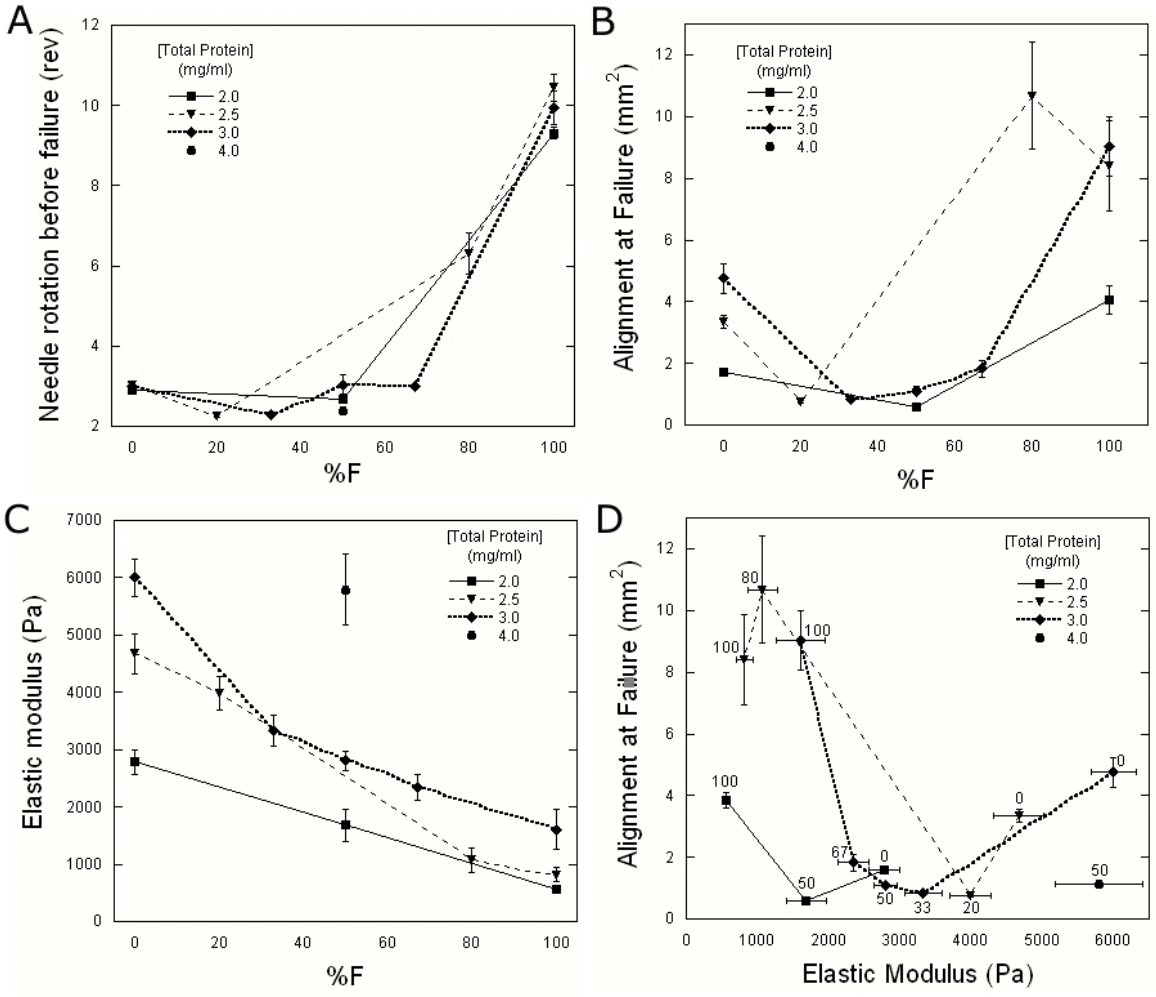

Figure 4-3. Effects of gel composition on the elastic modulus, gel failure, and alignment at failure (average +/- standard error). Gels with low fibrinogen content failed at an earlier number of needle rotations than pure collagen gels (a). As the fibrinogen content was increased, gels were able to withstand more needle revolutions where pure fibrin gels sustained the largest number of needle revolutions. Since alignment was increased with number of needle rotations, gels with relatively high fibrin content were able to last more needle rotations, which allowed gels to have higher level of alignment at failure (b). Elastic modulus was found decreased with increasing fibrinogen content within gels (c). Since alignment increased non-linearly with needle rotations, softer gels, which tend to last more needle rotations than stiffer gels, had relatively higher alignment at failure (d). Numbers next to the data plotted are gel compositions.

4.3.1.3 Mechanical stiffness

Micromechanical testing showed gels elastic moduli were decreased with increasing relative fraction of fibrin (Figure 4-3c), where collagen gels were significantly stiffer than

fibrin gels at the same total protein content. The effect of concentration on the elastic modulus within collagen or fibrin gels was statistically significant (ANOVA, $P<0.001$), where elastic modulus was found increased with protein concentration.

As previously mentioned, stiffer gels tend to fail at fewer rotations than softer gels. Lasting additional needle rotations allowed softer composite gels to reach relatively higher alignment at failure (Figure 4-3d and 4-4).

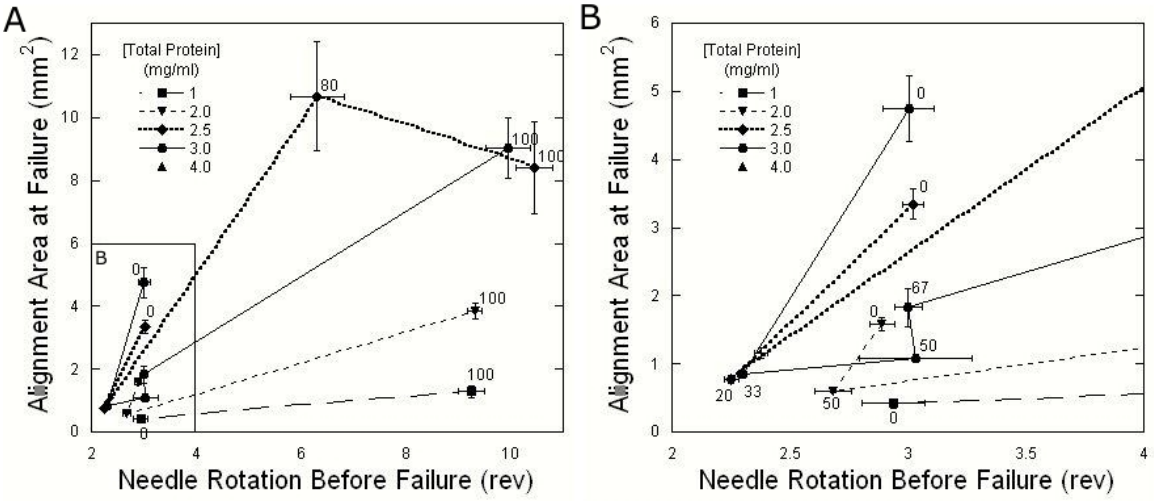

Figure 4-4. Alignment area at failure with respect to needle rotation before failure (average +/- standard error). Gels with relatively high fibrin content were able to withstand higher number of needle rotations resulting in larger amount of alignment area at failure compare to lower fibrin content gels at the same total protein content (A). Within the same composition gels (0%F), concentration effect was observed where alignment at failure was increased with protein concentration (B). Number next to the data plotted represented gel compositions.

4.3.2 Collagen – HA Composite Gels

4.3.2.1 Alignment

Using the same PLM, the '4-leaf clover' patterns were observed in HA- collagen composite gels during needle rotation. As in previous results (Chapter 3), we observed a significant effect of gel geometry on fiber alignment (ANOVA, $P<0.001$), where smaller gels aligned more than larger gels (Figures 4-5). In general, the alignment area was found increasing with the number of needle revolutions. For the same number of revolutions, the average alignment area was decreased with increasing HA concentration, with and without PPE ring. However, the effect of concentrations on the alignment was statistically significant only when comparing between groups of 0 and 2mg/ml HA concentration (Tukey's test, $P < 0.001$).

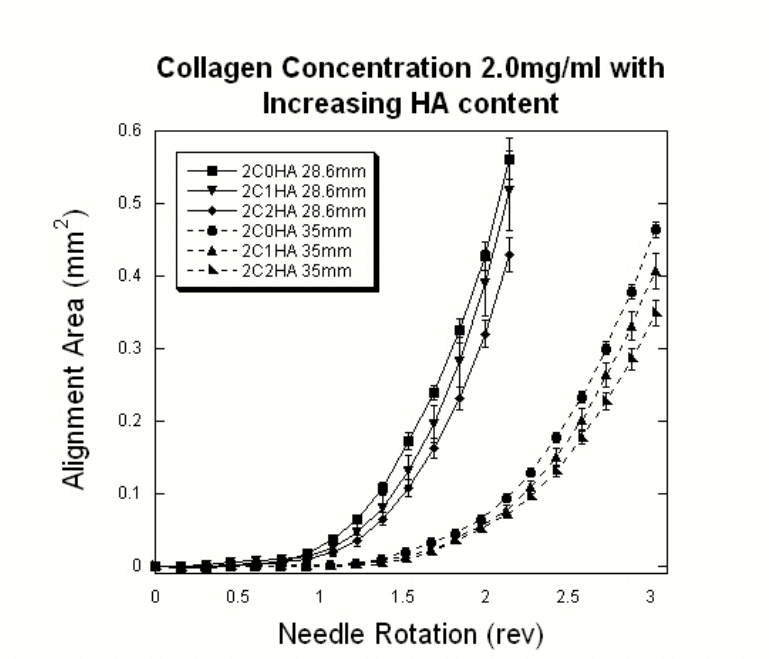

Figure 4-5. Effects of HA on the alignment area within 28.6mm and 35mm gels (average +/- standard error). The birefringent area of an alignment was identified from image sets binarized based on the image at 2 revolutions, and plotted as a function of needle revolution. In general, alignment was decreased with increasing HA concentration. C: [Collagen](mg/ml), HA: [Hyaluronic Acid] (mg/ml).

4.3.2.2 Gel failure

Similar to the previous chapter, we observed and effect of gel geometry of the ability for the gels to withstand needle rotation, where smaller gels failed at fewer needle rotations than larger gels (ANOVA, P<0.001) (Figure 4-6a). As the HA concentration was increased, gels failed at a later number of needle revolutions. The effect of concentration on gel failure was only statistically significant between groups of 0mg/ml and 2mg/ml HA concentration (Tukey's test, P < 0.001).

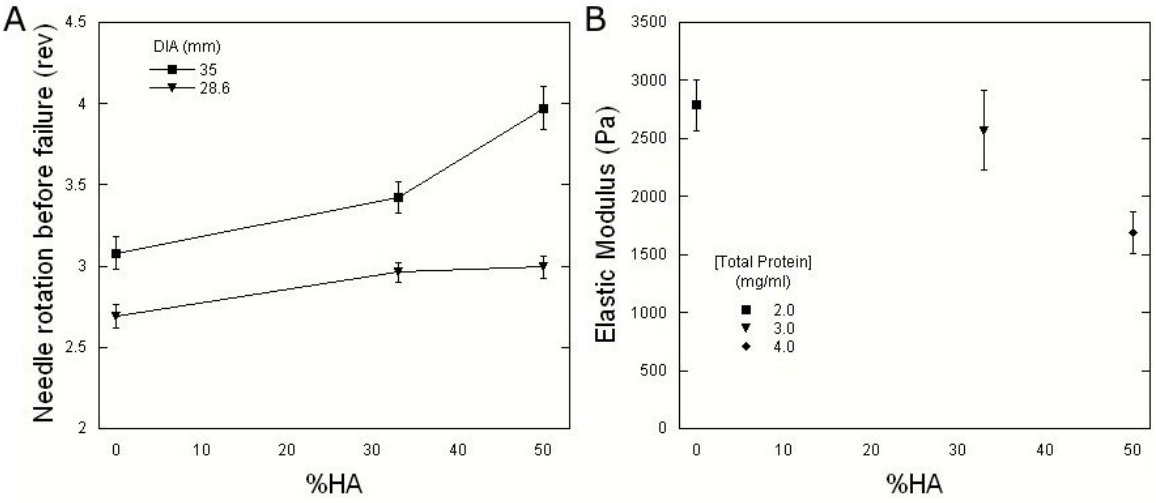

Figure 4-6. Effects of gel composition on the gel failure (a) and the elastic modulus (b) (average +/- standard error). The effect of gel geometries on gel failure was significant (ANOVA, P<0.001). Increasing HA concentration within HA-collagen composite gels increased the number of needle rotation before failure (a), but decreased the elastic modulus (b). Tukey's method indicates the effect of concentration on gel failure is only significant between groups of 0mg/ml and 2 mg/ml (P<0.001), and is insignificant on elastic modulus (P=0.132).

4.3.2.3 Mechanical stiffness

Increasing the concentration of HA within a collagen gel decreased the stiffness, but the results were not statistically significant (ANOVA, P=0.132). Thus, even though the effect

of concentrations at 2mg/ml HA showed significant effect on both the alignment and the gel failure (Tukey's, $P<0.001$), we cannot correlate the gel failure as well as the alignment to the stiffness.

4.4 Discussion

Using the in vitro acupuncture setup, we tried to understand the role of tissue properties in the immediate mechanical responses related to tissue grasp and tissue alignment. We also found that changing composition has a major effect on the gel's mechanical properties. We have previously shown (Chapter 2) that stiffness changes induced by crosslinking decreased the alignment and the gel failure point. Changes produced by increasing total collagen content (without crosslinking) affected alignment, but not failure. We were interested in examining how changes in tissue composition would change the response to in vitro acupuncture, and whether those changes were consistent with our previous results regarding stiffness. In general, stiffer gels were prepared increasing the total protein concentration and/or collagen content of composite gels.

We found that at the same number of needle rotations, within gels with the same amount of total protein, alignment area was found highest in collagen gels, lowest in fibrin gels, and composite gels were in between. Composites with relatively higher collagen content had higher alignment area. We believed that the difference in the alignment mainly due to the natural birefringence capability of collagen and fibrin fibers. We made our composite gels similar to previously constructed collagen-fibrin gels by Rowe and Stegemann. However, our thrombin concentration was 10 times higher which might result in much

shorter and finer fibrin fibers compared to collagen fibers [11]. Finer fibrin fibers might have led to a much lower alignment in fibrin gels. However, we used fluorescence microscopy to observe collagen and fibrin fibers in our composite gels. There was no major difference in fiber diameters under 63x-objective. Nevertheless, we observed gels with relatively higher collagen content and higher elastic modulus had higher alignment area at the same number of needle rotations. Hence, alignment response might be due to fibril properties, where less compliant fibers, collagen, were able to align faster but failed at much earlier number of needle rotations and more compliant fibers, fibrin, caused gels to withstand additional needle rotations resulting in higher alignment at failure. Hence, as fibrin content was increased within composite gels with relatively low collagen content, gels tend to behave similarly to pure fibrin gels. We also found that inclusion of fibrin in collagen gels decreased the stiffness of gels. We believed that collagen fibers generally play a dominant role in gel failure only when the concentration within composite gels is at least 1mg/ml. Once collagen content dropped to 0.5mg/ml (eg 80%F in a gel comprising 2.5 mg/ml total protein concentration), composite gels behaved similar to pure fibrin gels in terms of both failure and alignment.

On the other hand, collagen gels containing HA had lower alignment area compared to pure collagen gels. Electron microscopy has shown that HA forms a globular coat on collagen fibers and nano fiber connections between collagen fibers [15]. When looking at fluorescently labeled collagen and HA-collagen composite gels, we observed similar increases in fiber spacings as mentioned in Turley's work. However, later work by Reid and Newman reported that there was no difference in pore size between collagen with

and without HA [16]. Regardless of the space increase, our findings of alignment decreased with increasing HA concentration may be due to the globular coating on fibers and the nano-fibers formed in between the collagen fibers which might have minimized collagen birefringence. If indeed there is a space increase, the additional spacing between fibers might delay the fiber winding and reduce the alignment response. However, at our working concentrations, we were not able to show the correlation between gel stiffness and gel failure as in collagen-fibrin results and previous studies (chapter 2). Nevertheless, we showed that indeed, incorporation of either fibrinogen (fibrillar form) or HA (globular form) to collagen affect the alignment response. The effect of HA concentration may not be significant at 1mg/ml, but at 2m/ml, significant effects was shown. The significance of HA concentration may be enhanced by further increasing the concentration to 4mg/ml or more.

From this study, we showed how in vitro system can be modified systematically and still capture the basic characteristics in actual tissues. We believe that our in vitro set up enables the study of acupuncture mechanism in both quantitative and controlled manners which may be difficult for in vivo and in situ studies. We were able to capture the effect of gel compositions and gel properties on the needling response.

As mentioned, acupuncturists generally insert a needle into the skin and manipulated until de qi is reached. There is no specific numbers of needle rotations for a specific therapy. The manipulation is generally stopped when the tugging sensation as a result of tissue grasping on the needle is felt by the acupuncturists. Hence, unlike prescription in

western medicine, there is no specific correlation between number of needle rotations and therapeutic effects. Since tissue composition varies with age, sex, and the location through out the body [8], we believed that patient's tissue conditions may affect the outcome of the therapy. The amount of winding to reach de qi would vary between patients. If a therapeutic effect requires certain amount of tissue alignment, patients with higher collagen contents in their tissues would require less needle manipulation, whereas patients with less responsive tissue contents would require more needle manipulations.

One of many difficulties in clinical studies to show the efficacy of acupuncture is to have a proper control. It is difficult to prevent patient feeling the needle insertion, which might cause placebo effect. As mentioned, the immediate response of acupuncture needling is tissue deformation. Connective tissue seems to be the key element in acupuncture mechanism. When forces required in removing inserted needles were measured, it was found that pull out forces were higher at acupuncture points compare to control points [6]. Nevertheless, there were minor responses at control points which might lead to placebo effects. If indeed, connective tissues hold the key to acupuncture mechanism, any changes to tissue properties including tissue compositions and mechanical properties will affect the ultimate therapeutic response. Hence, it is difficult to have a proper control due to variance between patients during clinical studies unless patients' tissue compositions are known prior to acupuncture application. Further understanding and studies of tissue compositions are definitely needed.

We believe that we shed some light into the significance of tissue properties, where patient to patient variability may be the main reason most clinical studies remain inconclusive. More importantly, we have a system that is easily modified to study the basic mechanism behind the acupuncture therapy.

4.5 References

1. Birch, S., et al., *Clinical research on acupuncture. Part 1. What have reviews of the efficacy and safety of acupuncture told us so far?* J Altern Complement Med, 2004. **10**(3): p. 468-80.
2. Statement, N.C., *Acupuncture*. 1997, NIH.
3. Langevin, H.M., et al., *Subcutaneous tissue fibroblast cytoskeletal remodeling induced by acupuncture: evidence for a mechanotransduction-based mechanism.* J Cell Physiol, 2006. **207**(3): p. 767-74.
4. Langevin, H.M., et al., *Dynamic fibroblast cytoskeletal response to subcutaneous tissue stretch ex vivo and in vivo.* Am J Physiol Cell Physiol, 2005. **288**(3): p. C747-56.
5. Langevin, H.M., et al., *Connective tissue fibroblast response to acupuncture: dose-dependent effect of bidirectional needle rotation.* J Altern Complement Med, 2007. **13**(3): p. 355-60.
6. Langevin, H.M., et al., *Biomechanical response to acupuncture needling in humans.* J Appl Physiol, 2001. **91**(6): p. 2471-8.
7. Langevin, H.M. and J.A. Yandow, *Relationship of acupuncture points and meridians to connective tissue planes.* Anat Rec, 2002. **269**(6): p. 257-65.
8. Vitellaro-Zuccarello, L., et al., *Stereological analysis of collagen and elastic fibers in the normal human dermis: variability with age, sex, and body region.* The Anatomical Record, 1994. **238**(2): p. 153-62.
9. Hsu, S., A.M. Jamieson, and J. Blackwell, *Viscoelastic studies of extracellular matrix interactions in a model native collagen gel system.* Biorheology, 1994. **31**(1): p. 21-36.
10. Pretorius, E., *The role of alternative and complementary treatments of asthma.* Acupunct Electrother Res, 2009. **34**(1-2): p. 15-26.
11. Rowe, S.L. and J.P. Stegemann, *Interpenetrating collagen-fibrin composite matrices with varying protein contents and ratios.* Biomacromolecules, 2006. **7**(11): p. 2942-8.
12. Shreiber, D., P. Enever, and R. Tranquillo, *Effects of PDGF-BB on rat dermal fibroblast behavior in mechanically stressed and unstressed collagen and fibrin gels.* Experimental Cell Research, 2001. **266**: p. 155-166.
13. Julias, M., et al., *An in vitro assay of collagen fiber alignment by acupuncture needle rotation.* Biomed Eng Online, 2008. **7**: p. 19.
14. Lin, D.C., B. Yurke, and N.A. Langrana, *Use of rigid spherical inclusions in Young's moduli determination: application to DNA-crosslinked gels.* J Biomech Eng, 2005. **127**(4): p. 571-9.
15. Turley, E.A., C.A. Erickson, and R.P. Tucker, *The retention and ultrastructural appearances of various extracellular matrix molecules incorporated into three-dimensional hydrated collagen lattices.* Dev Biol, 1985. **109**(2): p. 347-69.
16. Reid, G.G. and I. Newman, *Human leucocyte migration through collagen matrices containing other extracellular matrix components.* Cell Biol Int Rep, 1991. **15**(8): p. 711-20.

5. DISCUSSION AND FUTURE WORK

During acupuncture therapy, needles are inserted into skin and manipulated to achieve “de qi”. As mentioned, from the therapists perspective, de qi is a biomechanical phenomenon involving connective tissues, which wind and wrap around the needle resulting in needle grasp [1, 2]. Initially, the in vitro system developed in this work was aimed at capturing the basic structural components of loose connective tissues involved in acupuncture. We began with acellular collagen gels, which allowed us to show the effect of collagen concentration and crosslinking on needling response. We observed stiffer crosslinked collagen gels failed at fewer number of needle rotations than untreated collagen gels, where crosslinking decreased the alignment. This indicates that mechanical properties of connective tissues affect the response to acupuncture needling. Loose connective tissue has been shown to have substantially different mechanical properties than some of the tissues that do not couple the needles during acupuncture - particularly dermis [3, 4], which paralleled our crosslinking results.

Furthermore, tissue thickness varies. Using different gel thickness, we captured different tissue thicknesses and we were able to vary different needle depth insertions. We found that both absolute and relative needle depth insertions are important factors in the alignment response. Alignment increased with needle depth insertion mostly due additional collagen fibers that couple to the needle. In general, alignment occurs at any gel thickness. This might pose problems in vivo or in clinical trials. Not only there might be placebo effect due to minor response at control points, but the response at control

points also varies depending on the tissue thickness at which the control points are located.

Meanwhile, the difference observed in alignment from separate batches of collagen showed that subtle changes in tissue composition and structure may affect the needling response. For the purpose of the study, where needle insertion is the particular parameter of interests, we believe that having the changes due to separate collagen batches will not affect the outcome of the alignment trend. However, the batch-to-batch differences, which might be due to impurities, may be eliminated by additional purification or purchasing the purer forms of the collagen used.

We further modeled fascial planes by changing the geometry of our collagen gels. We were able to capture the asymmetry of fascias where we observed the effect of gel geometries on needling response. The enhancement of alignment response due to specific gel geometries indicates that acupuncture utilizes fascia geometries as part of its mechanism. Since mechanical stimulation from acupuncture needle rotation stimulates resident fibroblasts [5, 6], enhancement by means of tissue properties and tissue boundaries may play important roles in acupuncture therapeutic effects.

Additionally, we showed the effect of tissue compositions and their properties on the alignment response. We were able to modify our in vitro system to capture basic changes of HA content in tissues [7] by changing HA concentration within in vitro gels, where we showed effects of compositions on gel stiffness and the alignment response. Varying gel

compositions clearly affected the outcome of needling, which lead us to believe that differences in tissue contents between patients might have caused variation in therapeutic outcomes. By understanding the significance of matrix composition, we might be able to decrease the discrepancy of therapeutic effects from patient to patient, or identify patient populations that are more amenable to acupuncture therapy. If there is a specific level of mechanical signals required by residing cells to achieve therapeutic effects, patients with more compliant tissues might need additional number of needle rotations to achieve the same level of tissue deformation compare to patients with tissues that are less susceptible to needling.

As our understanding of the elements involved in mechanical coupling during acupuncture therapy improves, we can begin to understand what is happening at the cellular level during acupuncture needling. When we incorporated fibroblasts within our collagen gels, we observed the cell alignment and fibroblasts expanded morphology after 2 needle revolutions. As mentioned, mechanical stress as a result of acupuncture needling caused morphological changes [5, 6], which might activate signaling cascades leading to cellular responses such as cell contraction, migration, protein synthesis, and cellular effects including cell proliferation, cell survival, cell differentiation, and cell death due to modification of the surrounding ECMs [3, 8-10]. These events may further affect neighboring cells and the surrounding matrix, resulting in further remote effects through the dendritic network of fibroblasts [11]. Nevertheless, the role of expanded morphology on acupuncture therapeutic effects remains to be elucidated. In chapter 3, cells were found following the orientation of matrix alignment as a result of needle rotation.

Downstream effects of the mechanical needle rotations remain to be elucidated. With our in vitro system, cell types and cell densities can be modified to explore the effect of needling on cellular behaviors. Understanding important processes, such as proliferation and cell migration via direct or indirect acupuncture needling may be useful in engineering applications including wound healing and nerve regeneration.

Meanwhile, acupuncture, although currently an 'alternative therapy', has been shown effective in treating dermatological diseases with fewer side effects, at which could have been prevented with proper techniques and education [9]. Case studies showed commonly used treatments (skin grafting, laser therapy, varicose vein surgery, and specialist dressings) had no effects on patients until the application of acupuncture [12, 13]. Studies have shown that acupuncture provokes peripheral vasodilation in skin and muscles, which is believed to be one of the reasons behind the latter's efficacy [12, 14].

An in vitro system might provide a platform to study the mechanism behind the efficacy of acupuncture in treating scars, ulcer, or other skin diseases. For example, a case study [13] where a patient suffered from wounds that were unable to heal, needles were inserted at various locations (>15 acupuncture points). Regardless of wound locations, two of the wounded areas had one needle particularly inserted close to wound perimeters [13] (Figure 5-1a). There seemed to be no needling near the parietal wound. It is interesting to understand the significance of needling locations specifically in wound healing applications. As mentioned, the extent of cellular responses depends on specific mechanical stimulus [6]. Using 3D in vitro gels, we can mimic the basic wound

characteristics (Figure 5-1b) and understand the significance of needling locations during acupuncture applications. We may shed some light to the specificity of acupuncture points with the corresponding therapeutic effects and determine the specific magnitude of tissue manipulations to reach optimal, fibroblasts induced, gel compaction within different gel components.

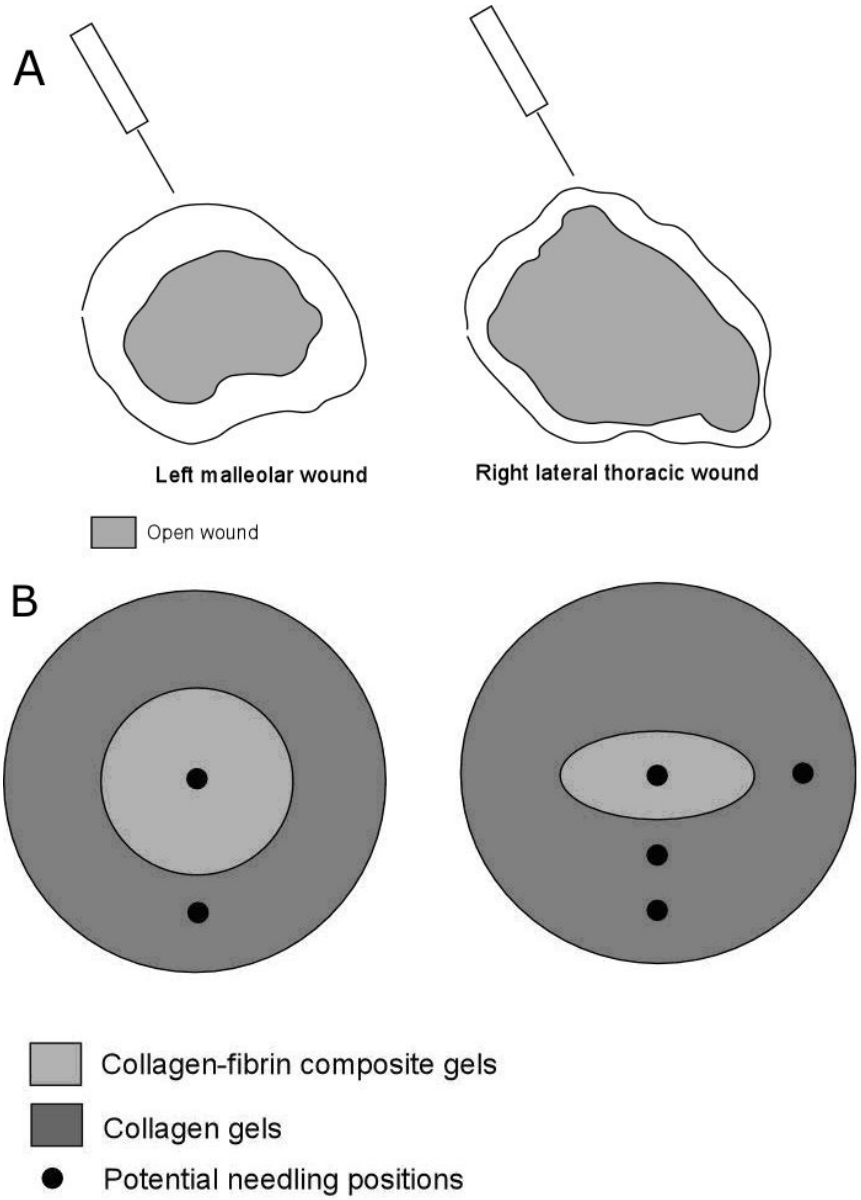

Figure 5-1. In vitro model capturing basic wound characteristics. Schematic of left malleolar and right lateral thoracic wounds indicating locations at which acupuncture

needling were applied closely to the wound periphery [13] (A). Gel within another gel can be used to understand the significance of needling locations during a wound healing application using acupuncture (B). Inner gel, consists of collagen-fibrin composites, can be used to represent open wound areas, whereas stiffer outer gel can be used to mimic the outer skin perimeter. Needles can be inserted and rotated at different locations to observe the effect of needling positions on the alignment response.

Additionally, rarely, acupuncture therapy involves only insertion of a single needle . Typically, acupuncture therapy involves multiple needles insertions at various locations. We showed the effect of boundary conditions on alignment response. If needle rotations create circumferential alignment near the needle and radial alignment at further locations, the circumferential alignment may act as a boundary with respect to the second needle, and so on (Figure 5-2). With the in vitro system, the effect of additional needles on the alignment pattern can be studied. Understanding the significance of multiple needles insertions during therapy will be a step further in shedding some light on acupuncture mechanism, i.e. whether multiple needling enhances mechanical stimulation remotely.

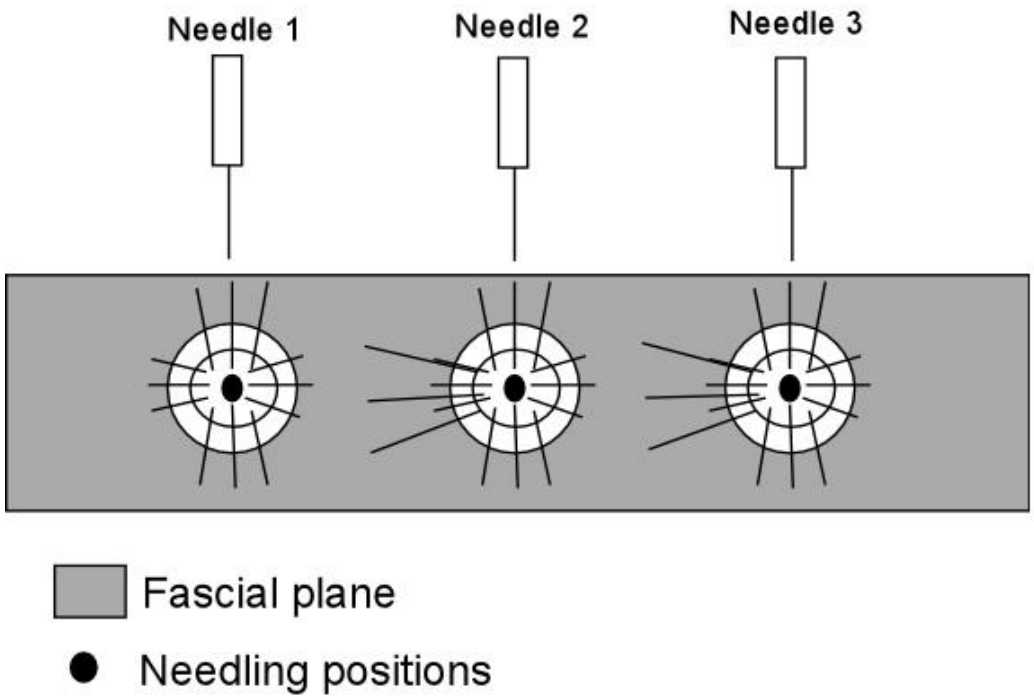

Figure 5-2. Effects of multiple needles insertions on the alignment response. First needle insertion will result in alignment response as shown in the previous chapter, where alignment is stronger at minor axis than at major axis. After the first needle insertion and manipulation, the resulting gel deformations act as a boundary to the second needle as it is manipulated. Stronger alignment will occur not only at minor axis, but also at the location where boundary is created by the first needling. Similar phenomenon might occur for additional needles. Multiple needles insertions may enhance the alignment not only across the fascia, but also along the entire length (major axis) of the fascial plane.

Nevertheless, there is always a limitation in each therapy. As an example, skin grafting can only be applied when the wound is well vascularized [15]. In addition, patients respond differently to applied treatments. Hence, an alternative or modifications of current treatments are always needed. With proper understanding of acupuncture mechanism, we may be able to improve its effectiveness or even utilize its technique for other engineering applications.

A potential application might be in cancer screening. Tumor generations remain unclear until recent studies, which showed the correlation between collagen content and tumor proliferation [16]. The purpose of Barnes' work was to show a potential novel mechanical testing tool to analyze tissue that is relatively small for current available methods. The size of biopsies seems to be a constraint that is difficult to overcome. Although farfetched, there might be a potential use in studying tissue mechanical properties using acupuncture needling. Since gel failures can be correlated with corresponding mechanical properties, tissue mechanical properties can be interpreted by inserting a needle into the tissue and manipulating it afterwards.

In closing, we have shown the effect of compositions and mechanical properties on needling response. We also showed the role of fascia geometry and needling parameter in the alignment response. As we improve the image capturing rate, we might be able to capture effects of higher needle rotational speeds and viscoelasticity on the needling response. Additionally, we believe that modification and improvement to the in vitro system with mechanical sensors, which allow the measurement of applied forces and torques as a gel is manipulated in vitro, will provide important information that will strengthen our in vitro studies and more importantly allow the further understanding of underlying mechanism of acupuncture.

5.1 References

1. Langevin, H.M. and J.A. Yandow, *Relationship of acupuncture points and meridians to connective tissue planes.* Anat Rec, 2002. **269**(6): p. 257-65.
2. Langevin, H.M., et al., *Biomechanical response to acupuncture needling in humans.* J Appl Physiol, 2001. **91**(6): p. 2471-8.
3. Langevin, H.M., et al., *Evidence of connective tissue involvement in acupuncture.* Faseb J, 2002. **16**(8): p. 872-4.
4. Iatridis, J.C., et al., *Subcutaneous tissue mechanical behavior is linear and viscoelastic under uniaxial tension.* Connect Tissue Res, 2003. **44**(5): p. 208-17.
5. Langevin, H.M., et al., *Subcutaneous tissue fibroblast cytoskeletal remodeling induced by acupuncture: evidence for a mechanotransduction-based mechanism.* J Cell Physiol, 2006. **207**(3): p. 767-74.
6. Langevin, H.M., et al., *Connective tissue fibroblast response to acupuncture: dose-dependent effect of bidirectional needle rotation.* J Altern Complement Med, 2007. **13**(3): p. 355-60.
7. Hsu, S., A.M. Jamieson, and J. Blackwell, *Viscoelastic studies of extracellular matrix interactions in a model native collagen gel system.* Biorheology, 1994. **31**(1): p. 21-36.
8. Langevin, H.M., D.L. Churchill, and M.J. Cipolla, *Mechanical signaling through connective tissue: a mechanism for the therapeutic effect of acupuncture.* Faseb J, 2001. **15**(12): p. 2275-82.
9. Iliev, E., *Acupuncture in dermatology.* Clin Dermatol, 1998. **16**(6): p. 659-88.
10. Guido, S. and R.T. Tranquillo, *A methodology for the systematic and quantitative study of cell contact guidance in oriented collagen gels. Correlation of fibroblast orientation and gel birefringence.* J Cell Sci, 1993. **105 (Pt 2)**: p. 317-31.
11. Langevin, H.M., C.J. Cornbrooks, and D.J. Taatjes, *Fibroblasts form a body-wide cellular network.* Histochem Cell Biol, 2004. **122**(1): p. 7-15.
12. Mears, T., *Acupuncture for chronic venous ulceration.* Acupunct Med, 2003. **21**(4): p. 150-2.
13. Diogenes, M.S., A.C. Carvalho, and A.M. Tabosa, *Acupuncture and moxibustion as fundamental therapeutic complements for full recovery of staphylococcal skin infection after a poor 50-day treatment response to antibiotics.* J Altern Complement Med, 2008. **14**(6): p. 757-61.
14. Vas, J., et al., *Effectiveness of acupuncture, special dressings and simple, low-adherence dressings for healing venous leg ulcers in primary healthcare: study protocol for a cluster-randomized open-labeled trial.* BMC Complement Altern Med, 2008. **8**: p. 29.
15. Braddock, M., C.J. Campbell, and D. Zuder, *Current therapies for wound healing: electrical stimulation, biological therapeutics, and the potential for gene therapy.* Int J Dermatol, 1999. **38**(11): p. 808-17.
16. Barnes, S.L., P.P. Young, and M.I. Miga, *A novel model-gel-tissue assay analysis for comparing tumor elastic properties to collagen content.* Biomech Model Mechanobiol, 2009. **8**(4): p. 337-43.

Bibliography

(2002). "World Health Organization. Acupuncture: Review and analysis of reports on controlled trials." (Geneva: WHO).

(2005). "Acupuncture in oncology practice and research." J Soc Integr Oncol 3(4): 166-76.

Abe, M., M. Takahashi, et al. (2003). "The changes in crosslink contents in tissues after formalin fixation." Analytical Biochemistry 318: 118-123.

Ahn, A. C., J. Wu, et al. (2005). "Electrical impedance along connective tissue planes associated with acupuncture meridians." BMC Complement Altern Med 5: 10.

Almog, J., Y. Cohen, et al. (2004). "Genipin-a novel fingerprint reagent with colorimetric and fluorogenic activity." J Forensic Sci 49(2): 255-7.

Atance, J., M. Yost, et al. (2004). "Influence of the extracellular matrix on the regulation of cardiac fibroblast behavior by mechanical stretch." J. Cell. Physiol 200: 377-386.

Bank, R., M. Bayliss, et al. (1998). "Ageing and zonal variation in post-translational modification of collagen in normal human articular cartilage." The Biochemical Journal 330: 345-351.

Barnes, S. L., P. P. Young, et al. (2009). "A novel model-gel-tissue assay analysis for comparing tumor elastic properties to collagen content." Biomech Model Mechanobiol 8(4): 337-43.

Bell, E., B. Ivarsson, et al. (1979). "Production of a tissue-like structure by contraction of collagen lattices by human fibroblasts of different proliferative potential in vitro." Proc Natl Acad Sci U S A 76(3): 1274-8.

Berman, B. M., L. Lao, et al. (2004). "Effectiveness of acupuncture as adjunctive therapy in osteoarthritis of the knee: a randomized, controlled trial." Ann Intern Med 141(12): 901-10.

Birch, S., J. K. Hesselink, et al. (2004). "Clinical research on acupuncture. Part 1. What have reviews of the efficacy and safety of acupuncture told us so far?" J Altern Complement Med 10(3): 468-80.

Bouffard, N. A., K. R. Cutroneo, et al. (2007). "Tissue stretch decreases soluble TGF-beta1 and type-1 procollagen in mouse subcutaneous connective tissue: Evidence from ex vivo and in vivo models." J Cell Physiol.

Braddock, M., C. J. Campbell, et al. (1999). "Current therapies for wound healing: electrical stimulation, biological therapeutics, and the potential for gene therapy." Int J Dermatol 38(11): 808-17.

Bride, J., C. Viennet, et al. (2004). "Indication of fibroblast apoptosis during the maturation of disc-shaped mechanically stressed collagen lattices." Arch Dermatol Res 295: 312-317.

Bromage, T., H. Goldman, et al. (2003). "Circularly Polarized Light Standards for Investigations of Collagen Fiber Orientation in Bone." The Anatomical Record (Part B: New Anat) 274B(157-168).

Charlebois, M., M. McKee, et al. (2004). "Nonlinear Tensile Properties of Bovine Articular Cartilage and Their Variation With Age and Depth." Journal of Biomechanical Engineering 126(2): 129-37.

Da Silva, D., B. Vidal, et al. (2006). "Collagen birefringence in skin repair in response to red polarized-laser therapy." Journal of Biomedical Optics 11(2): 024002-1-6.
Debessa, C., L. Maifrino, et al. (2001). "Age related changes of the collagen network of the human heart." Mechanisms of Ageing and Development 122: 1049-1058.
Diogenes, M. S., A. C. Carvalho, et al. (2008). "Acupuncture and moxibustion as fundamental therapeutic complements for full recovery of staphylococcal skin infection after a poor 50-day treatment response to antibiotics." J Altern Complement Med 14(6): 757-61.
Dubey, N., P. Letourneau, et al. (2001). "Neuronal contact guidance in magnetically aligned fibrin gels: effect of variation in gel mechano-structural properties." Biomaterials 22: 1065-1075.
Eckes, B., C. Mauch, et al. (1993). "Downregulation of collagen synthesis in fibroblasts within three-dimensional collagen lattices involves transcriptional and posttranscriptional mechanisms." FEBS 318(2): 129-133.
Eisenberg, D., R. Davis, et al. (1998). "Trends in alternative medicine use in the United States, 1990-1997." JAMA 280(18): 1569-1575.
Elsdale, T. and J. Bard (1972). "Collagen substrata for studies on cell behavior." J Cell Biol 53(3): 626-637.
Eshel, H. and Y. Lanir (2001). "Effects of strain level and proteoglycan depletion on preconditioning and viscoelastic responses of rat dorsal skin." Ann Biomed Eng 29(2): 164-72.
Girton, T., V. Barocas, et al. (2002). "Confined compression of a tissue-equivalent: collagen fibril and cell alignment in response to anisotropic strain." Journal of Biomechanical Engineering 124: 568-575.
Gogly, B., G. Godeau, et al. (1997). "Morphometric analysis of collagen and elastic fibers in normal skin and gingiva in relation to age." Clin Oral Invest 1: 147-152.
Goldman, H., T. Bromage, et al. (2003). "Preferred Collagen Fiber Orientation in the Human Mid-shaft Femur." The Anatomical Record Part A 272A: 434-445.
Grinnell, F. (2003). "Fibroblast biology in three-dimensional collagen matrices." Trends in Cell Biology 13(5): 264-269.
Grinnell, F., C. Ho, et al. (2003). "Dendritic fibroblasts in three-dimensional collagen matrices." Molecular Biology of the Cell 14: 384-395.
Guido, S. and R. T. Tranquillo (1993). "A methodology for the systematic and quantitative study of cell contact guidance in oriented collagen gels. Correlation of fibroblast orientation and gel birefringence." J Cell Sci 105 (Pt 2): 317-31.
Hammerschlag, R., P. D. Culliton, et al. (2003). "A new partnership: the Society for Acupuncture Research and the Journal of Alternative and Complementary Medicine." J Altern Complement Med 9(6): 807-8.
He, Y. and F. Grinnell (1994). "Stress relaxation of fibroblasts activates a cyclic AMP signaling pathway." J Cell Biology 126(2): 457-464.
Hsu, S., A. M. Jamieson, et al. (1994). "Viscoelastic studies of extracellular matrix interactions in a model native collagen gel system." Biorheology 31(1): 21-36.
Iatridis, J. C., J. Wu, et al. (2003). "Subcutaneous tissue mechanical behavior is linear and viscoelastic under uniaxial tension." Connect Tissue Res 44(5): 208-17.
Iliev, E. (1998). "Acupuncture in dermatology." Clin Dermatol 16(6): 659-88.

Jacques, S., J. Roman, et al. (2000). "Imaging Superficial Tissues With Polarized Light." Lasers in Surgery and Medicine 26: 119-129.

Jing, Y. and Y. Jian-Xiong (2009). "Human tissue factor pathway inhibitor-2 suppresses the wound-healing activities of human Tenon's capsule fibroblasts in vitro." Mol Vis 15: 2306-12.

Julias, M., L. T. Edgar, et al. (2008). "An in vitro assay of collagen fiber alignment by acupuncture needle rotation." Biomed Eng Online 7: 19.

Kaptchuk, T. J. (2002). "Acupuncture: theory, efficacy, and practice." Ann Intern Med 136(5): 374-83.

Kessler, D., S. Dethlefsen, et al. (2001). "Fibroblasts in mechanically stressed collagen lattices assume a "synthetic" phenotype." J Biol Chem 276(39): 36575-85.

Knapp, D. M., E. F. Helou, et al. (1999). "A fibrin or collagen gel assay for tissue cell chemotaxis: assessment of fibroblast chemotaxis to GRGDSP." Exp Cell Res 247(2): 543-53.

Konofagou, E. E. and H. M. Langevin (2005). "Using ultrasound to understand acupuncture. Acupuncture needle manipulation and its effect on connective tissue." IEEE Eng Med Biol Mag 24(2): 41-6.

Kucharz, E. (1992). The Collagens: Biochemistry and Pathophysiology.

Kung, Y., F. Chen, et al. (2005). "Convulsive Syncope: An Unusual Complication of Acupuncture Treatment in Older Patients." J Altern Complement Med 11(3): 535-537.

Langevin, H. M., G. J. Badger, et al. (2004). "Yin scores and yang scores: A new method for quantitative diagnostic evaluation in traditional Chinese medicine research." J Altern Complement Med 10(2): 389-95; discussion 387.

Langevin, H. M., N. A. Bouffard, et al. (2006). "Subcutaneous tissue fibroblast cytoskeletal remodeling induced by acupuncture: evidence for a mechanotransduction-based mechanism." J Cell Physiol 207(3): 767-74.

Langevin, H. M., N. A. Bouffard, et al. (2005). "Dynamic fibroblast cytoskeletal response to subcutaneous tissue stretch ex vivo and in vivo." Am J Physiol Cell Physiol 288(3): C747-56.

Langevin, H. M., N. A. Bouffard, et al. (2007). "Connective tissue fibroblast response to acupuncture: dose-dependent effect of bidirectional needle rotation." J Altern Complement Med 13(3): 355-60.

Langevin, H. M., D. L. Churchill, et al. (2001). "Mechanical signaling through connective tissue: a mechanism for the therapeutic effect of acupuncture." Faseb J 15(12): 2275-82.

Langevin, H. M., D. L. Churchill, et al. (2001). "Biomechanical response to acupuncture needling in humans." J Appl Physiol 91(6): 2471-8.

Langevin, H. M., D. L. Churchill, et al. (2002). "Evidence of connective tissue involvement in acupuncture." Faseb J 16(8): 872-4.

Langevin, H. M., C. J. Cornbrooks, et al. (2004). "Fibroblasts form a body-wide cellular network." Histochem Cell Biol 122(1): 7-15.

Langevin, H. M., R. Hammerschlag, et al. (2006). "Controversies in acupuncture research: selection of controls and outcome measures in acupuncture clinical trials." J Altern Complement Med 12(10): 943-53.

Langevin, H. M., E. E. Konofagou, et al. (2004). "Tissue displacements during acupuncture using ultrasound elastography techniques." Ultrasound Med Biol 30(9): 1173-83.

Langevin, H. M., D. M. Rizzo, et al. (2007). "Dynamic morphometric characterization of local connective tissue network structure in humans using ultrasound." BMC Syst Biol 1: 25.

Langevin, H. M. and K. J. Sherman (2007). "Pathophysiological model for chronic low back pain integrating connective tissue and nervous system mechanisms." Med Hypotheses 68(1): 74-80.

Langevin, H. M., K. N. Storch, et al. (2006). "Fibroblast spreading induced by connective tissue stretch involves intracellular redistribution of alpha- and beta-actin." Histochem Cell Biol 125(5): 487-95.

Langevin, H. M. and P. D. Vaillancourt (1999). "Acupuncture: does it work and, if so, how?" Semin Clin Neuropsychiatry 4(3): 167-75.

Langevin, H. M. and J. A. Yandow (2002). "Relationship of acupuncture points and meridians to connective tissue planes." Anat Rec 269(6): 257-65.

Le, J., A. Rattner, et al. (2002). "Production of matrix metalloproteinase 2 in fibroblast reaction to mechanical stress in a collagen gel." Arch Dermatol Res 294(9): 405-10.

Lin, D. C., B. Yurke, et al. (2005). "Use of rigid spherical inclusions in Young's moduli determination: application to DNA-crosslinked gels." J Biomech Eng 127(4): 571-9.

Mays, P., R. McAnulty, et al. (1995). "Age-related Alterations in Collagen and Total Protein Metabolism Determined in Cultured Rat Dermal Fibroblasts: Age-related Trends Parallel those Observed in Rat Skin In Vivo." Int. J. Biochem. Cell Biol. 27(9): 937-945.

Mears, T. (2003). "Acupuncture for chronic venous ulceration." Acupunct Med 21(4): 150-2.

Miura, M., E. Elsner, et al. (2005). "Imaging Polarimetry in Central Serous Chorioretinopathy." Am J Opthalmol 140(6): 1014-1019.

Mudera, V., R. Pleass, et al. (2000). "Molecular responses of human dermal fibroblasts to dual cues: contact guidance and mechanical load." Cell Motility and the Cytoskeleton 45: 1-9.

Murray, M. M., S. D. Martin, et al. (2000). "Migration of cells from human anterior cruciate ligament explants into collagen-glycosaminoglycan scaffolds." J Orthop Res 18(4): 557-64.

Ng, C. P. and M. A. Swartz (2003). "Fibroblast alignment under interstitial fluid flow using a novel 3-D tissue culture model." Am J Physiol Heart Circ Physiol 284(5): H1771-7.

Oxlund, H., J. Manschot, et al. (1988). "The role of elastin in the mechanical properties of skin." J Biomech 21(3): 213-8.

Peleg, R., H. Gotshal, et al. (2005). "Patterns of Use of Nonbiomedical Medicine Services by Nonbiomedical Medicine Providers." J Altern Complement Med 11(5): 917-921.

Pierce, M., J. Strasswimmer, et al. (2004). "Birefringence measurements in human skin using polarization-sensitive optical coherence tomography." Journal of Biomedical Optics 9(2): 287-291.

Pleis, J. R. and J. W. Lucas (2009). "Summary health statistics for U.S. adults: National Health Interview Survey, 2007." Vital Health Stat 10(240): 1-159.

Pretorius, E. (2009). "The role of alternative and complementary treatments of asthma." Acupunct Electrother Res 34(1-2): 15-26.

Reid, G. G. and I. Newman (1991). "Human leucocyte migration through collagen matrices containing other extracellular matrix components." Cell Biol Int Rep 15(8): 711-20.

Rowe, S. L. and J. P. Stegemann (2006). "Interpenetrating collagen-fibrin composite matrices with varying protein contents and ratios." Biomacromolecules 7(11): 2942-8.

Sasazaki, Y., R. Shore, et al. (2006). "Derformation and failure of cartilage in the tensile mode." Journal of Anatomy 208(6): 681-694.

Shreiber, D., P. Enever, et al. (2001). "Effects of PDGF-BB on rat dermal fibroblast behavior in mechanically stressed and unstressed collagen and fibrin gels." Experimental Cell Research 266: 155-166.

Silver, F. H., D. DeVore, et al. (2003). "Invited Review: Role of mechanophysiology in aging of ECM: effects of changes in mechanochemical transduction." J Appl Physiol 95(5): 2134-41.

Smalls, L., R. Wickett, et al. (2006). "Effect of dermal thickness, tissue composition, and body site on skin biomechanical properties." Skin Research and Technology 12: 43-49.

Statement, N. C. (1997). Acupuncture, NIH. 15(5).

Stegemann, J. and R. Nerem (2003). "Phenotype modulation in vascular tissue engineering using biochemical and mechanical stimulation." Annals of Biomedical Engineering 31(4): 391-402.

Sung, H., W. Chang, et al. (2003). "Crosslinking of biological tissues using genipin and/or carbodiimide." J Biomed Mater Res 64A: 427-438.

Sung, H., Y. Chang, et al. (1999). "Crosslinking characteristics and mechanical properties of a bovine pericardium fixed with a naturally occurring crosslinking agent." J Biomed Mater Res 47: 116-126.

Takahashi, M., H. Hoshino, et al. (1995). "Direct Measurement of Crosslinks, Pyridinoline, Deoxypyridinoline, and Pentosidine, in the Hydrolysate of Tissues Using Hign-Performance Liquid Chromatrography." Analytical Biochemistry 232: 158-162.

Tham, L. M., H. P. Lee, et al. (2006). "Cupping: from a biomechanical perspective." J Biomech 39(12): 2183-93.

Tower, T., M. Neidert, et al. (2002). "Fiber Alignment Imaging During Mechanical Testing of Soft Tissues." Annals of Biomedical Engineering 30: 1221-1233.

Turley, E. A., C. A. Erickson, et al. (1985). "The retention and ultrastructural appearances of various extracellular matrix molecules incorporated into three-dimensional hydrated collagen lattices." Dev Biol 109(2): 347-69.

Varani, J., M. Dame, et al. (2006). "Decreased Collagen Production in Chronologically Aged Skin." American Journal of Pathology 168(6): 1861-1868.

Vas, J., M. Modesto, et al. (2008). "Effectiveness of acupuncture, special dressings and simple, low-adherence dressings for healing venous leg ulcers in primary healthcare: study protocol for a cluster-randomized open-labeled trial." BMC Complement Altern Med 8: 29.

Vidal, B. (2003). "Image analysis of tendon helical superstructure using interference and polarized light microscopy." Micron 34: 423-432.

Vishwanath, V., K. Frank, et al. (1986). "Glycation of skin collagen in type I diabetes mellitus. Correlation with long-term complications." Diabetes 35(8): 916-21.

Vitellaro-Zuccarello, L., S. Cappelletti, et al. (1994). "Stereological analysis of collagen and elastic fibers in the normal human dermis: variability with age, sex, and body region." The Anatomical Record 238(2): 153-62.

Vogel, H. (1980). "Influence of maturation and aging on mechanical and biochemical properties of connective tissue in rats." Mechanisms of Ageing and Development 14(3-4): 283-92.

Wozniak, M., K. Modzelewska, et al. (2004). "Focal adhesion regulation of cell behavior." Biochimica et Biophysica Acta 1692: 103-119.

Yamamura, N., R. Sudo, et al. (2007). "Effects of the Mechanical Properties of Collagen Gel on the In Vitro Formation of Microvessel Networks by Endothelial Cells." Tissue Engineering 14(7): 1-11 (page numbers are temporary).

Yarrow, J. C., Z. E. Perlman, et al. (2004). "A high-throughput cell migration assay using scratch wound healing, a comparison of image-based readout methods." BMC Biotechnol 4: 21.

Zeng, Y., A. Qiao, et al. (2003). "Collagen fiber angle in the submucosa of small intestine and its application in gastroenterology." World Journal of Gastroenterology 9(4): 804-807.

Zhang, H., L. Sun, et al. (2006). "Quantitative analysis of fibrosis formation on the microcapsule surface with the use of picro-sirius red staining, polarized light microscopy, and digital image analysis." Journal of Biomedical Materials Research Part A 76A(1): 120-125.

CURRICULUM VITA

Margaret Julias

Education:

January 2010	Rutgers, The State University of New Jersey Ph.D. Chemical and Biochemical Engineering "An In Vitro Assay for Acupuncture: Effects of Gel Composition, Properties, and Geometry on the Alignment Response"
January 2007	Rutgers, The State University of New Jersey M.S. Chemical and Biochemical Engineering
May 2003	Rutgers, The State University of New Jersey B.S. Chemical Engineering Minors: Chemistry and Mathematics

Position:

December 2009	Teaching Assistant Rutgers, Dept. of Biomedical Engineering
May 2009	Graduate Assistant Rutgers, Dept. of Chemical and Biochemical Engineering
May 2007	NJ Center of Spinal Cord Research - fellow Rutgers, Dept. of Chemical and Biochemical Engineering
May 2005	Teaching Assistant Rutgers, Dept. of Chemical and Biochemical Engineering
August 2004	NJ Center of Biomaterials - Summer fellow Rutgers, Dept. of Chemical and Biochemical Engineering
May 2004	Graduate Assistant Rutgers, Dept. of Chemical and Biochemical Engineering
August 2003	Co-Op Colgate – Palmolive Technology Center, Piscataway, NJ

Publications:

Julias M, Edgar LT, Buettner HM, Shreiber DI. An in vitro assay of collagen fiber alignment by acupuncture needle rotation. BioMedical Engineering OnLine 2008, 7:19.

Julias M, Buettner HM, Shreiber DI. Varying assay geometry to emulate connective tissue planes in an in vitro model of acupuncture. In Review 2009.

Julias M, Buettner HM, Shreiber DI. Effects of assay compositions on acupuncture needle rotation. Manuscript in preparation 2009.